On-line Residual Capacity Estimation for Resource Allocation in Wireless Mesh Networks

by Yunus Sarikaya

Submitted to the Graduate School of Sabancı University
in partial fulfillment of the requirements for the degree of
Master of Science

Sabanci University

August, 2008

APPROVED BY

Assist. Prof. Dr. Özgür Gürbüz .....
(Thesis Supervisor)

Assist. Prof. Dr. Özgür Erçetin .....
(Thesis Co-supervisor)

Assist. Prof. Dr. Kerem Bülbül .....

Assoc. Prof. Dr. Albert Levi .....

Assoc. Prof. Dr. Erkay Savaş .....

DATE OF APPROVAL: .....

Abstract

Contention-based multi access scheme of 802.11 based wireless mesh networks imposes difficulties in achieving predictable service quality in multi-hop networks. In order to offer effective advanced network services such as flow admission control or load balancing, the residual capacity of the wireless links should be accurately estimated.

In this work, we propose and validate an algorithm for the residual bandwidth of wireless mesh network. By collecting transmission statistics from the nearby nodes that are one and two hops away and by using a basic collision detection mechanism, the packet delivery failure probability for a given link is estimated. The packet failure probability is used in an analytical model to calculate the maximum allowable traffic level for this link in saturation condition.

We evaluate the efficacy of the method via OPNET simulations, and show that the percent estimation error is significantly lower than a recent prominent estimation method; i.e. error is between 0.5-1.5%. We demonstrate that flow admission control is successfully achieved in a realistic WMN scenario based on accurate link residual bandwidth estimates. A flow control algorithm based on residual bandwidth keeps the unsatisfied traffic demand bounded and at a negligibly low level. We also propose a routing metric that uses residual bandwidth as link metric and we show that this routing algorithm results in a significant increase in network throughput compared to other popular metrics.

Özet

802.11 dayal kablosuz rg şebekelerin rekabete dayalı çoklu erişim şemaları, çok atlamalı şebekelerde tahmin edilebilir servis kalitesi kazandırmada zorluklar içermektedir. Akış kabul kontrolu veya yük dengesi gibi etkin gelişmiş şebeke servisleri sunmak için, kablosuz bağlantıların arta kalan kapasiteleri doğru olarak tahmin edilmelidir.

Bu çalışmada kablosuz mesh şebekelerinin arta kalan bant genişliği iin algoritma sunuyoruz ve geçerliğini kontrol ediyoruz. lk olarak bir veya iki atlama uzaklıktaki yakın nodlardan iletim istatistiklerini toplayarak verilmiş bir bağlantı için paket ulaştırma hatası olasılığı hesaplanıyor. Bu paket ulaştırma hatası olasılığı, analitik bir model içerisinde doygunluk durumundaki bir bağlantı için maksimum izin verilen trafik seviyesinin hesaplanması sırasında kullanılıyor.

Metodun etkinliği OPNET simulasyonları aracılığıyla değerlendiriyoruz ve yüzde tahmin hatasının yeni ve ünlü tahmin metodunkinden önemli ölçüde az olduğunu gösteriyoruz: hata 0.5-1.5% arasında. Doğru bağlantı arta kalan bant genişliğine dayanan akış kabul kontrolu gerçek WMN senaryoları için başarılı olarak uygunlandığını gösteriyoruz. Arta kalan bant genişliğine dayanan akış kabul kontrolu, yerine getirelememiş trafik isteğini ihmal edilebilecek kadar düşük düzeyde tutuyor. Ayrıca bağlantı metriği olarak kullanılan arta kalan bant genişliğini, rota tespit etme metriği olarak öneriyoruz ve diğer popüler metriklere nazaran karşılandırıldığında bu rota tespit etme algoritmasının şebeke throughput'unda önemli ölçüde artışa neden olduğunu gösteriyoruz.

Acknowledgements

I wish to express my gratitude to my advisor Asst. Prof. Özgür Gürbüz for her valuable guidance, patience and understanding throughout my studies at Sabanci University. I am also very grateful to my co-advisor Asst. Prof. Özgür Erçetin for his inspiring ideas and support during my studies.

It was great pleasure for me working with all the members of Networking Lab. I thank my friends for their cooperation and companionship. I would like to thank to the members of the jury of my thesis; Assist. Prof. Dr. Albert Levi, Assist. Prof. Dr. Erkay Savaş and Assist. Prof. Dr. Kerem Bülbül for spending their valuable time.

I would like to thank TÜBİTAK, for providing the necessary motivation and funding.

Lastly, I am grateful to my family for their endless love, understanding and patience that made me follow my own path.

Contents

List of Figures

List of Tables

1 Introduction

With the proliferation of 802.11 based wireless networks, people expect the same service quality from those networks that they experience over broadband wired networks. A key step in the provisioning of better quality of service (QoS) is to correctly estimate the traffic handling capacities of the wireless network links or paths. The difference between network link (or path) capacity and the current load of the system identifies the additional user demand that can be satisfied, which is known as the *residual bandwidth* as previously discussed in the literature within the framework of ad hoc wireless networks [1], [2],[3]. Despite existing work, accurate estimation of residual bandwidth in 802.11 based wireless multi-hop networks, such as Wireless Mesh Networks (WMNs), without causing extra overhead is still an open problem. Dynamically changing wireless medium characteristics due to varying user traffic patterns and channel conditions jeopardize the precision of the bandwidth estimation process. In order to obtain a good estimate of residual bandwidth, transmission activity on the channel should be tracked perfectly and on time while causing as little disruption to the network operation as possible.

In this work, we provide a generalized analysis of the wireless link capacity under realistic network conditions and mesh network scenarios. This work differs from those available in the literature, since it combines real measurements with analytical calculations and considers all possible circumstances which affect the residual bandwidth. These circumstances include the effects of different link rates and packet sizes, channel impairments, topology asymmetries and hidden nodes. In fact, this is why our residual bandwidth estimation method is so powerful, resulting in an average percentage estimation error as low as 1%. Since our algorithm does not make any assumptions about the network topology, it can be used in any wireless mesh scenario based on 802.11 access. Also, the measurements utilized by our algorithm are simply obtained

by overhearing the transmitted frames and by exchanging small packets with neighbors, which significantly reduces the overhead compared to other residual bandwidth algorithms that use probe packets. Moreover, due to low complexity and real-time and distributed operation, our algorithm can be easily applied in practical mesh networks with simple updates in each wireless node.

The residual bandwidth estimation mechanism can be utilized in advanced network services and resource allocation, such as admission control and efficient routing. In admission control, we determine whether a path would meet the throughput demand of a newly arriving flow by considering the estimated residual bandwidth, and in routing, we aim to choose the path with the highest residual bandwidth, which not only provides QoS but also balances the load in the network. We show that accurate estimation provided by our proposed method also results in significant improvement in performance of those network services due to effective resource allocation.

1.1 Contributions

The key contributions of this thesis are:

• Analytical formulation of the residual bandwidth estimation process considering IEEE 802.11 based WMNs, multi-hop communication, fading and flow asymmetry.

• Obtaining the residual bandwidth correctly with introducing minimum overhead into the network.

• Low computational complexity of the proposed residual bandwidth estimation algorithm.

• Demonstration of network performance improvements by using residual bandwidth in applications such as flow admission control and routing.

1.2 Thesis Organization

The rest of the thesis is organized as follows: Section II provides a brief summary of DCF and the challenges of calculating residual bandwidth in 802.11 based wireless networks, and summarizes the earlier studies. Section III defines network model and introduces theory behind residual bandwidth estimation. Section IV presents our analytical model with details of modeling busy period, idle period and calculation of loss probability. Section V introduces the simulation environment, OPNET, and explains some key features of the models. Section VI provides performance analysis for the proposed algorithm, including estimation accuracy, convergence and complexity analysis, and applications in admission control and routing. Section VII concludes our work by summarizing the contributions of this thesis.

2 BACKGROUND

2.1 IEEE 802.11 Based Wireless Mesh Networks

Wireless Mesh Networks are composed of wireless access points (routers) that facilitates the connectivity and intercommunication of wireless clients through multi-hop wireless paths by routing packets. The mesh may be connected to the Internet through gateway routers or mesh portals.

Unlike Mobile Ad hoc Networks (MANETs) where every routing node is mobile, routing nodes (mesh nodes) in mesh networks are stationary. Clients, which are mobile nodes with no routing capability, connect to the mesh nodes and use the backbone to communicate with one another over large distances and with nodes on the Internet. In addition to mesh networking among mesh routers and mesh clients, the gateway/bridge functionalities in mesh routers enable the integration of WMNs with various other networks.

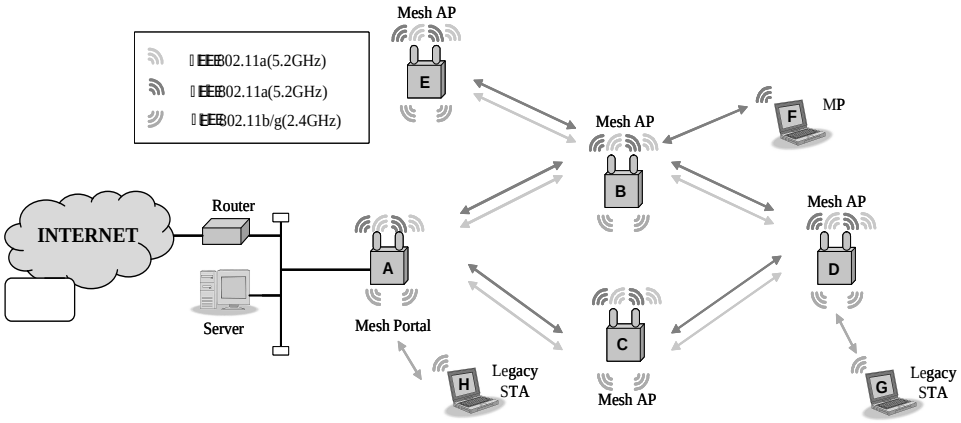

Figure 1: Wireless mesh architecture

Many advantages of WMNs appear as a consequence of its architecture. First advantage is that the mesh is self-configuring. New nodes can become

members of the mesh topology automatically as soon as the nodes after entering into the mesh. Secondly, a wireless mesh network delivers scalable performance because it can be expanded easily and incrementally as needed. In addition, wireless access points provide connectivity and robustness which is not always achieved with mobile and selfish clients in MANETs. Because of these advantages, WMNs can be used in applications such as home networks, community networks, metropolitan area networks, and enterprise networks.

Wireless mesh networks offer great potential to enhance wireless networking. Thus, many researchers and companies have already realized the potential of this technology and concentrate their efforts on WMNs. Researchers have started to revisit the protocol design and enhancements of existing wireless networks, especially of IEEE 802.11 networks. In this work, we focus on 802.11 based WMNs and its capacity estimation.

2.2 Distributed Coordination Function (DCF)

The primary access method of IEEE 802.11, called Distributed Coordination Function (DCF), is basically a Carrier Sense Multiple Access with Collision Avoidance (CSMA/CA) mechanism [4]. In DCF, a station desiring to transmit monitors the channel activity. If the channel is idle for a period of time equal to a distributed inter-frame space (DIFS), the station transmits directly. If the medium is busy (i.e. transmissions are taking place by other transmissions), then the station defers its transmission until the channel becomes idle. After that, the station waits for a random period, which is determined by backoff procedure to avoid collisions. Fig. 2 illustrates the basic access mechanism of DCF.

Backoff procedure of 802.11 works as follows: If the channel is busy at first attempt, the station defers until the end of the transmission, which currently occupies the channel. After the deferring period, the number of the backoff

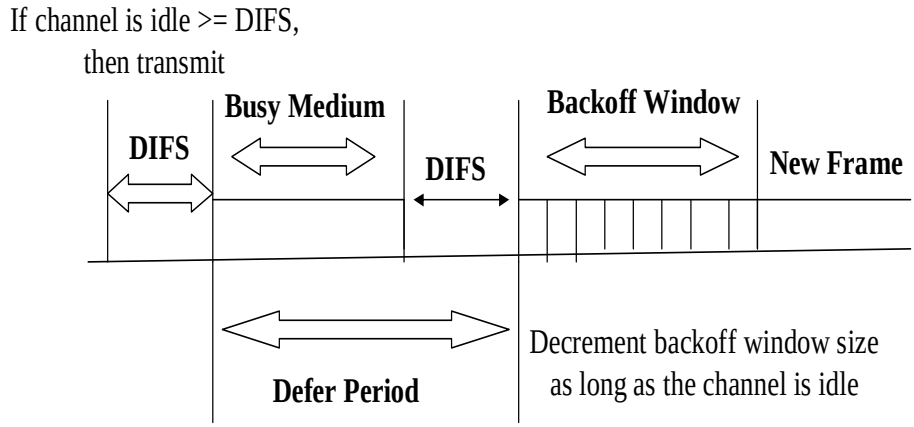

Figure 2: Basic Access Mechanism of DCF

time-slots is uniformly chosen from the range $(0, W_{min} - 1)$, where W_{min} is called minimum contention window size (one time-slot is equal to μ seconds) and backoff is started. The backoff time counter is decremented as long as the channel is sensed idle, frozen when a transmission is detected on the channel, and reactivated when the channel is sensed idle again for more than a DIFS. The station transmits when the backoff time reaches zero. For each unsuccessful transmission, the contention window is doubled, up to a maximum value $W_{max} = 2^m W_{min}$, where m is the retransmission limit.

An 802.11 DCF wireless link between a pair of source-destination nodes is considered as saturated when the MAC buffer in the source node always has at least one data packet waiting to be transmitted. Therefore, saturated links are always busy in the sense that they are either in backoff stage or actually transmitting a data packet. However if the MAC buffer in the source node becomes empty, this wireless link is considered as unsaturated. In unsaturated links, we typically have idle periods between consecutive transmissions where the system waits for new packet arrivals. A post-backoff scheme has been adopted in 802.11 DCF to handle empty MAC buffer situations. If a transmitter node

transmits all packets in its buffer and detects that its buffer is empty, it goes through a single post-backoff stage whose slot duration is randomly chosen from the range $(0, W-1)$. If there are new arrivals during the post-backoff stage, these packets are directly transmitted when post-backoff counter expires. If there are no new arrivals during this single post-backoff stage, the system waits for new arrivals without any further backoff process. As soon as a new arrival occurs in this particular state, the communication medium is sensed and if it is idle, the newly arrived packet is directly transmitted. If the communication medium is sensed as busy, the system proceeds with the standard backoff procedure. The DCF backoff scheme is illustrated in Fig. 3 as a flow chart.

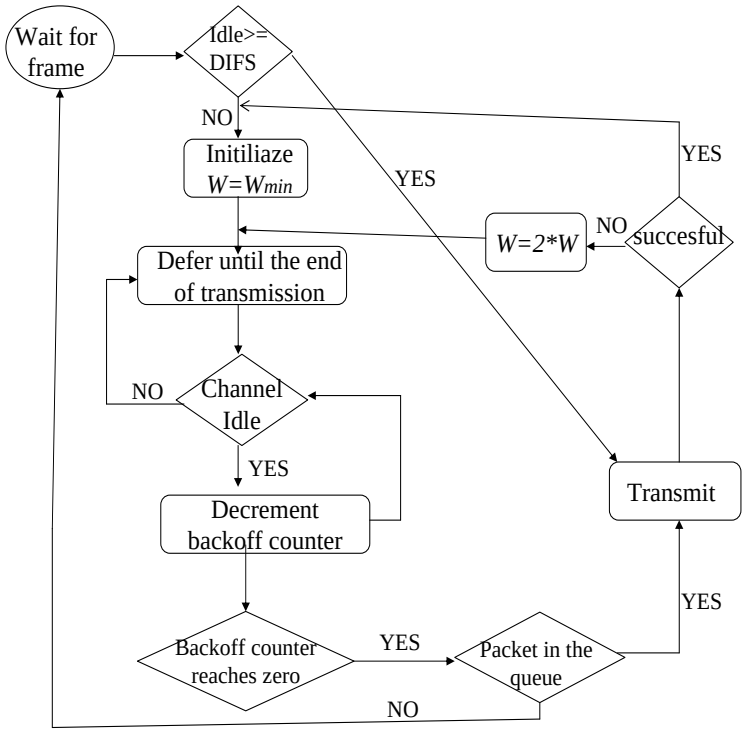

Figure 3: DCF Backoff Scheme

2.2.1 Challenges of DCF

Although DCF is designed to prevent collisions, it cannot completely eliminate them. There are mainly two causes to collisions: 1) Two stations simultaneously can send their packets even if they can sense each other. 2) There can be a hidden node sensed by the receiver of the link but it may not be sensed by the sender. An extension of DCF where nodes exchange RTS-CTS packets is proposed for hidden node problem, but this mechanism imposes significant overhead, and the problem cannot be completely solved [5].

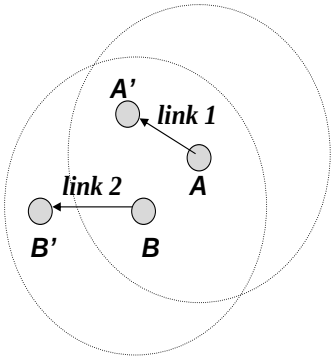

Figure 4: The example network for contention

Collisions between neighboring stations are the traditional type of losses due to MAC protocol used in DCF, which is able to coordinate transmissions of sources that are in the range of each other. In DCF, stations always listen to the channel and if there is an ongoing transmission, then they set their network allocation vector (NAV) and defer the transmission until the end of ongoing transmission to avoid collisions. However, if stations start their transmissions in the same slot, they cannot hear other's transmission due to being in transmitting state. As a result, a collision occurs between stations, which can sense their transmissions and start transmitting in the same slot. However, transmitting in the same slot is not adequate condition for collisions

to occur. The receivers should sense the transmission on the other links. For example, in Fig. 4, the source of link 1 (node A) and the source of link 2 (node B) are in the sensing range of each other, but even if node B's transmission may cause collision in link 1, the transmission on link 1 does not cause collision in link 2.

Collisions due to hidden node's transmission is different from the first one due to lack of coordination between hidden node and the source of the link, which cannot sense hidden node's transmission. Thus, the collision takes place when the hidden node or the source of the link starts transmitting while the other one is still transmitting. The Request To Send (RTS)/Clear To Send (CTS) mechanism is also applied to solve the hidden node problem and increases the probability of successful transmission. However, the station cannot send the packets to others after receiving the RTS or the CTS frame because it must set the its NAV (Network Allocation Vector) and defer the transmission to avoid collision. Once the NAV counts down to zero, the station can re-contend to send the packets. Such a situation would increase the transmission delay and waste the radio resource, which is scarce in the wireless network. For that reason, even if RTS/CTS exchange partially solve the hidden node problem, it cannot eliminate the problem completely and it offers significant overhead, which reduces the network performance. We disable RTS/CTS mechanism and analyze hidden node problem without it.

Another challenge in DCF is the starvation of some wireless links, which occurs whenever a sender senses the activity of two or more other flows that do not sense each other. This phenomenon is called the Flow-in-the-Middle (FIM) problem. In FIM problem, the contending links of the middle flow may randomly overlap in time. Thus, the amount of time channel is seen as busy by the link in the middle is significantly lower as compared to the case in which all contending links can sense each others' transmissions. FIM is illustrated in

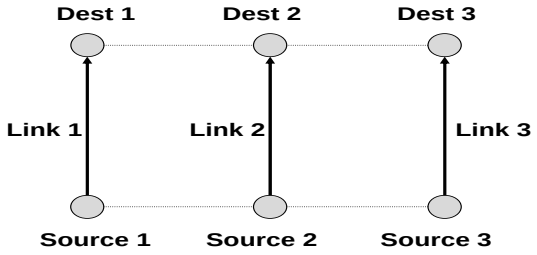

Figure 5: FIM Example

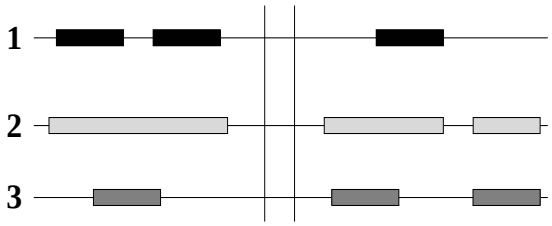

Figure 6: The channel activity of links 1 and 3 as sensed by the sender of link 2

Fig. 5. There are there links where two of them (link 1 and link 3) are out of range from each other. Link 2 cannot start transmission while other links are transmitting. However, as seen in Fig. 6, busy period seen by link 2 composes of overlaps between transmissions on link 2 and link 3.

2.3 Recent Work In Residual Bandwidth Estimation

A plethora of work have emerged on the issue of determining the residual bandwidth of DCF based wireless networks. These papers can fundamentally be classified into three categories, as passive, active (or intrusive) and analytical methods. Passive methods are based on monitoring the channel to obtain some important parameters, which are then used to estimate the bandwidth. One popular method is the "listen method" in which the physical radio channel ac-

tivity is recorded during an update period and observed statistics are utilized in computing the proportion of time the channel is idle [6, 7]. A host estimates its available bandwidth for new data transmissions as the channel bandwidth times the ratio of idle time to overall time, divided by a weight factor. The weight factor is introduced due to the nature of IEEE 802.11. The DIFS, SIFS, and backoff scheme represent overhead, which must be accounted for in each data transmission. However, the value of the weight factor is not specified and different weight factors are used in estimation, and an empirically assigned smoothing factor causes significant inaccuracies in residual bandwidth estimation process due to different 802.11 wireless network characteristics and time varying aspects of wireless communications.

Another passive approach is called the "time measurement" method [8], which is based on measuring the difference between the time a DATA packet leaves the MAC queue and the time its ACK is received as illustrated in Fig. 7. The measured delay is then normalized according to the packet size to obtain the residual bandwidth. The main drawback of both of these approaches is that they do not consider the backoff times, busy periods and failure probabilities, which significantly affect the residual bandwidth in 802.11 links.

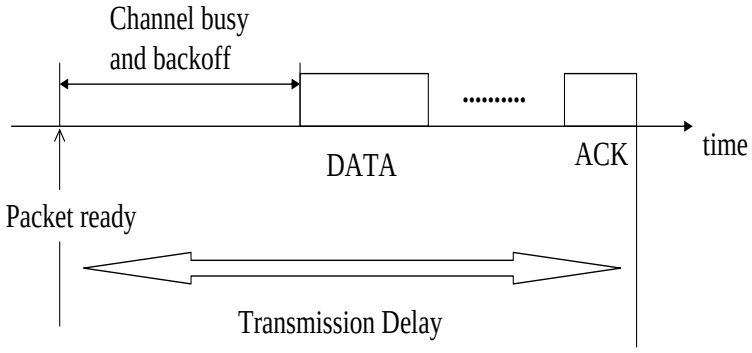

Figure 7: The transmission delay used in time measurement method

In active methods, the basic idea is to use very short probe packets sent at regular intervals between the source and the destination nodes [9, 10] or to use standard size end-to-end probe packets to saturate the wireless links and then estimate the residual bandwidth based on delay variation occurring just before the saturation point [11-13]. The first active method is called direct probing, where each probing stream results in a sample of the residual bandwidth. The sender transmits a periodic probing stream of specified rate, r_i and the receiver measures the output rate r_o. Residual bandwidth is calculated as:

$$RBW = C - r_i(\frac{C}{r_o} - 1), \tag{1}$$

where C is link capacity. However, the main assumption in the direct probing approach is that the link capacity C is known.

Another active approach is called iterative probing, in which it is not necessary to know the capacity of the estimated link. The sender transmits a periodic probing stream k with rate $r_i(k)$. The rate $r_i(k)$ varies either linearly, or as a function of the outcome of previous streams. If the k^{th} stream gives $r_o(k) < r_i(k)$, then we know that $r_i(k) > RBW$; otherwise, it is $r_i(k) \leq RBW$. The basic idea is that, through a sequence of streams with different rates, iterative probing can converge to the residual bandwidth. A key point about iterative probing is that it does not sample parameters to calculate the residual bandwidth; instead, it only samples whether a rate is larger than the residual bandwidth or not.

Third active residual bandwidth estimation technique inserts "hello" packets to be exchanged between the neighboring nodes [3]. These packets carry locally obtained available bandwidth information to other nodes, so that potential contention levels can be deduced and then used in residual bandwidth estimation. A major drawback of all these active or intrusive methods is their large overhead due to extraneous probing packets. In addition, as previously mentioned, direct probing techniques require the knowledge of the link capac-

ity C, which is a crucial assumption. Moreover, iterative probing converges to a range of values rather than to a single value in residual bandwidth estimation process, therefore the accuracy of the method is low. In addition, convergence time of such methods is also large due to using large amount of probing packets, so they are vulnerable to the possible changes in transmission activities of surrounding stations.

More recently, analytical modeling of DCF has captured further interest among researchers. For example, several papers derive the capacity of 802.11 for single-hop networks [14-16]. These models involve some crucial assumptions and simplifications: Due to single hop assumption, all contenders can sense others' transmissions and hence coordinate their transmissions. However, this is not the case for WMNs, which can consist of multi-hop topologies. In these models, the contending links are assumed to be in saturation, which is not only invalid in most of the cases, but has significant impact on the collision probability as well. Models for multi-hop wireless networks come in varying degrees of analytical detail and topology assumptions. For example, [17] and [18] perform a detailed Markov chain analysis to determine the throughput, proposing a high complexity algorithm that is only limited to a specialized topology structure. [19] exploits the behavior of DCF to some extent, especially considering the binary exponential backoff mechanism together with FIM and hidden node problems, in contrast to the approaches in [20] and [21]. [19] assumes that topology information is known and given a set of nodes and a set of flows, a network is mapped into a contention graph. This contention graph is used to extract neighboring flows and hidden nodes. Neighboring contention leads up to busy periods in a given node and hidden node contention causes collisions. By using the contention graph, failure and busy probabilities are deduced. After that, channel utilization in a unit time is modeled to find the residual bandwidth. Unfortunately, the approach in [19]

does not take into account the coordination problems due to carrier sensing and collisions between neighboring nodes. In addition, hidden node collisions are only partially addressed, assuming that such collisions occur only during data transmission and ignoring collisions that may also take place during transmission of ACKs. In section V, we show that such problems play a dominant role in the accuracy of residual bandwidth estimation, especially for WMNs, where nodes are in general in a form of star topology.

Another recent analytical method, presented in [22], considers transmission activities in the neighbors, backoff duration and collision in the calculation of the residual bandwidth. The calculations are made in both receiver and sender side. First, the number of time units during which the medium is available for both receiver and sender in a measurement period are calculated and the calculated the available bandwidth is found as the product of these numbers in terms of unit time. Then, the collision probability and backoff durations are used to compute the residual bandwidth as:

$$RB_{final} = (1 - p)(1 - K)RB,$$

where p is the collision probability and K denotes backoff duration in unit time. Here, RB includes only busy period, but RB_{final} takes into account the collision probability and backoff durations together with the busy period. The problem of this method is the calculation of the collision probability, which is measured through sending Hello packets, which increases the overhead. In addition, the effect of the transmission activities on the neighboring links is not considered.

3 SYSTEM MODEL AND THEORY

3.1 Network Model

In this work, we focus on wireless mesh networks operating on a single frequency channel, where there are multiple contention domains. To model each contention domain, it is essential to study the behavior of an individual station based on its private view of the channel. Thus, we constitute our modeling framework based on channel state seen by a single source as the one exemplified in Fig. 8.

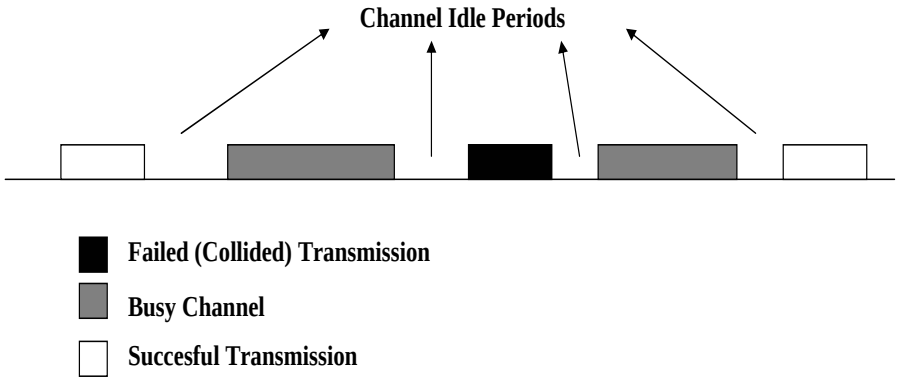

Figure 8: The channel view of individual station

There are four possible states of the channel that an individual station can observe: (1) the state that contains successful transmissions (2) idle channel state (3) busy channel state due to activity of other stations which compete to gain access to the channel (4) the channel state occupied by failed transmissions. In busy channel modeling, we consider FIM problem, which is not taken into account in most of the papers related to residual bandwidth calculation. For modeling the fraction of failed transmissions, channel errors due to fading,

failures due to hidden node collisions and collisions between neighboring links are all combined. In addition, the time spent for collisions between neighboring links is calculated under unsaturated conditions, which is one of the main contributions of this work, differentiating our algorithm from the method in [19].

3.2 Theoretical Basis of Residual Bandwidth Estimation

The residual bandwidth is mathematically defined as:

$$RB_i = C_i - f_i, \tag{2}$$

where C_i denotes the capacity of a link i and f_i is the current total flow on link i. We aim to minimize the estimation error of the residual bandwidth. Thus, our objective function is the mean square error between the actual and estimated residual bandwidth:

$$\min\ E(RB_i - \hat{RB_i})^2,$$

where RB_i and $\hat{RB_i}$ are the real and estimated residual bandwidth respectively. Our optimization problem is formulated as:

$$\begin{aligned}
&\min\ E(RB_i - \hat{RB_i})^2 \\
&\text{s.t. } f_i \geq \hat{C}_i \\
&\quad \hat{C}_i = g(\hat{T}^i_{idle}, \hat{T}^i_{busy}, \hat{p}^f_i) \\
&\quad \hat{T}^i_{idle} = h(\hat{p}^f_i) \\
&\quad \hat{T}^i_{busy} = y(N_j, T_j), \text{where } j \epsilon \nu(i) \\
&\quad \hat{p}^f_i = z(N_j, T_j, N_k, T_k), \text{where } j \epsilon \nu(i) \text{ and } k \epsilon \nu(j) \\
&\quad \hat{T}^i_{idle}, \hat{T}^i_{busy}, \hat{p}^f_i \geq 0.
\end{aligned} \tag{3}$$

Definitions of some of the variables are as follows:

$\nu(i)$: The neighbors of link i

$\hat{C}_i$: The estimated capacity of link i

$\hat{T}^i_{idle}$: The idle duration of link i

$\hat{T}^i_{busy}$: The busy duration of link i

$\hat{p}^f_i$: The failure probability of link i

N_j : The number of transmissions on link j in unit time

T_j : The total duration of transmission on link j in unit time.

The estimated capacity of a link, $\hat{C}_i$, is a function of three parameters, the idle period due to backoff times, $\hat{T}^i_{idle}$, which is directly proportional to the failure probability of that link, the busy periods due to transmission activities on the neighboring links of link i, which is defined as $\hat{T}^i_{busy}$, and the failure probability of that link, which is dependent on transmission activities in one hop and two hops neighbors such as the number of transmissions, N_j, the duration of transmissions, T_j, and channel quality.

The functions in (3) are implicit and they differ according to the algorithm used to find the residual bandwidth. According to non-linearity of these functions, it is hard to solve the optimization problem in closed form. For that reason, we first calculate the residual bandwidth by utilizing these functions and then we measure the estimation error. In section IV, the functions defined in (3) will be thoroughly explained and derived. In section VI, we will show that the estimation error is small enough and much lower than the error of current prominent residual bandwidth estimation algorithms.

3.3 Optimal Probabilistic Routing in Mesh Networks

Estimated capacity of a link can be utilized in many applications, such as, in load-balancing or finding optimal routes. In this section, we assume a wireless mesh network in which each node generates packets and sends them to the

base stations. It is assumed that the traffic generation rate and neighbors of each node in the network are known and network consists of M/M/1 queues. In such a network, we aim to minimize the total queuing delay in the network and the optimization formulation is:

$$\begin{aligned}
\min \quad & \sum_{P_w \epsilon P} \sum_{(i,j)\epsilon P_w} D_{ij}(P_{ij}) = \frac{\lambda_{ij}}{\mu_{ij} - \lambda_{ij}} \\
\text{s.t.} \quad & \sum_{(i,j)\epsilon OL(i)} P_{ij} = 1 \\
& \lambda_{ij} = (\sum_{(k,i)\epsilon L} \lambda_{ki} + \lambda_{0i}) P_{ij} \\
& \mu_{ij} = \frac{\alpha_{ij}(1 - \sum_{k\epsilon N(i)} \lambda_k \frac{L}{r})}{L/r} \\
& P_{ij} \geq 0 \\
& \mu_{ij} > \lambda_{ij}
\end{aligned} \tag{4}$$

The variables in (4) is as follows:

P_w : One path along a source-destination pair

P : The set contains all paths

L : Directed Link set

$OL(i)$: The links originated from node i

P_{ij} : Probability that the flow will go through link (i, j)(from node i to node j)

λ_{0i} : The arrival rate of packets originated from node i

λ_i : The arrival rate of packets at the node i

λ_{ij} : The arrival rate of packets on the link (i, j)

μ_{ij} : The service rate of the link (i, j), which is found in [23]

α_{ij} : The throughput of link (i, j) when it has no neighbors

$N(i)$: The set of neighbors of node i

L : Packet size

r : Physical data rate.

It is difficult to find a closed form solution for the optimal routing algorithm defined in (4) in terms of P_{ij}'s. We can only find the forwarding probability from node i to node j, P_{ij}, by using minimum search algorithms. The complexity of these search algorithms is directly proportional to the number of branches in the network. Thus, as the network size increases, the number of branches and so the complexity of search algorithm, is increased too, and optimal routing algorithm becomes insoluble in large networks. In addition, the optimal routing algorithm is centralized, where we need to know all transmission activities in the network. In section V, we show that a distributed min-max routing algorithm, which uses our residual bandwidth estimate as a metric, gets similar results with this optimal routing.

4 RESIDUAL BANDWIDTH ESTIMATION ALGORITHM

4.1 Algorithm Overview

The algorithm is designed to run in the sender node of the directed link named as the primary link, for which we would like to calculate residual bandwidth. The main inputs of the algorithm are: (1) the number of neighboring links, i.e., competing links, of the primary link (2) the number of packet deliveries per unit time on competing links (3) the packet failure rate for the primary link due to channel impairments. The number of competing links and their level of traffic are obtained by monitoring the DATA and ACK messages on the channel. Meanwhile, the packet failure rate of channel is deduced from the output of a basic collision detection scheme such as [24]. In multi-hop wireless networks, transmissions are mainly affected by the activities of the nodes that are one or two hops away. For this reason, in addition to one-hop neighbor's transmission information, the activities which are sensed by the competing links should be obtained. The sender of the competing link deduces all of its neighboring links' information by monitoring the channel, and shares this information (in form of successful packet transmissions(DATA or ACK) and failure probability) with its neighboring nodes by including them in HELLO packets of an existing routing protocol.

Table 1: The Parameters Utilized in RBW Estimation

	Parameter	Meaning
Measured	f_p	The current level of the traffic at the primary link
	N_i	The number of successful packet transmissions on the competing link i
	N_{h_i}	The number of successful packet transmissions on the hidden link i
	T_i^{tr}	Packet transmission time on competing link i
	T_p^{tr}	Packet transmission time on the primary link
	p_i^{fn}	Current failure probability of competing link i
	$\nu(i)$	the set of neighbors of link i
	$\eta(i,j)$	the set of common neighbors of link i and link j
	$\kappa(i)$	the set of hidden links of link i
Estimated	Np	The number of successful packet transmissions on the primary link
	p_p^f	Failure probability of the primary link
	p_i^f	Failure probability of competing link i
	T_p^{busy}	Busy Period for the primary link
	T_p^{idle}	Idle Period for the primary link
	T_i^{idle}	Idle Period for competing link i
	$p_i^t(s)$	Transmission probability of competing link i seen from the primary link
	$p_j^t(i)$	Transmission probability of competing link j seen from competing link i
	$p_p^t(i)$	Transmission probability of the primary link seen from competing link i
	$p_{h,i}^t(s)$	Transmission probability of hidden node i seen from the primary link
	$p_i^c(s)$	Pairwise collision probability between competing link i and the primary link
	$p_j^c(i)$	Pairwise collision probability between competing links i and j
	p_p^c	Collision probability of the primary link with the competing links
	p_p^h	Hidden node collision probability
	$p_{p,i}^h(s)$	Collision probability due to transmissions over hidden link i
	p_p^e	Loss probability due to fading

The essential parameters and notations referred in our analysis are listed in Table 1. The operation of our proposed algorithm is centered on a time sharing model, where the maximum number successful packet deliveries at the primary link is estimated under a hypothetical saturation condition. The basic operations of our algorithm is illustrated in Fig. 9. In order to obtain the residual bandwidth, we first determine idle period, which only consists of backoff times due to saturation assumption for the primary link. To find the idle period, we calculate the busy period of the primary link considering the

average transmission times of the competing links and overlapping periods. After determining idle period, we extract the first failure probability for the

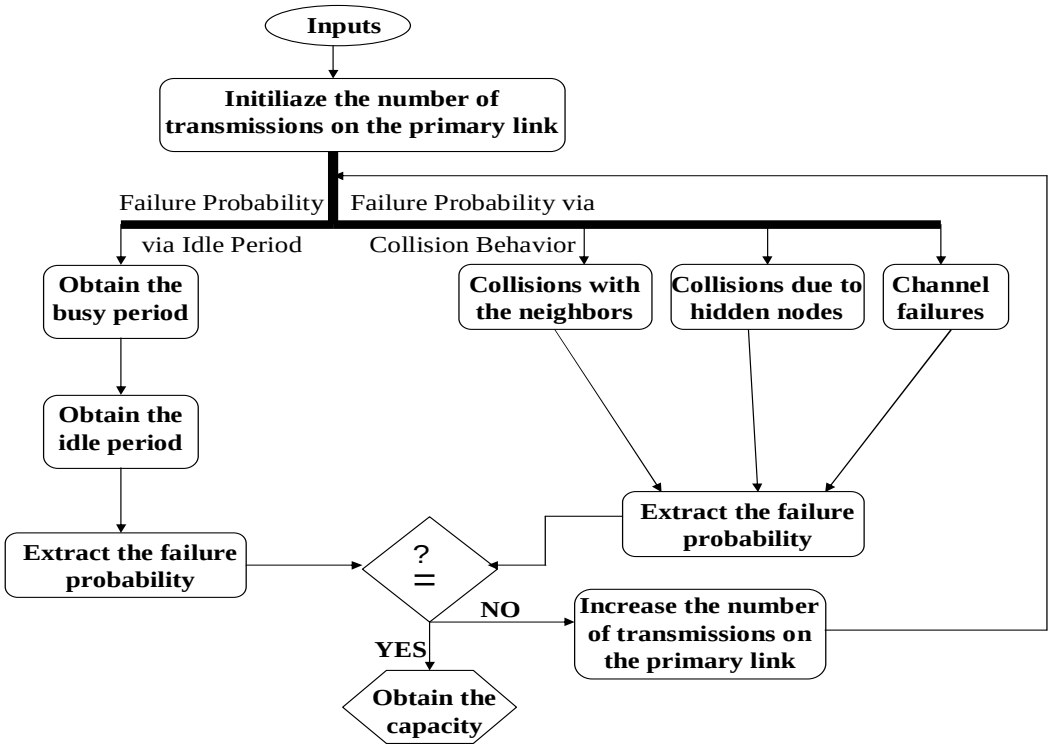

Figure 9: The basic flow chart of our RBW estimation algorithm

primary link by using the behavior of DCF backoff procedure. The second failure probability is obtained by incorporating packet failures due to channel errors, hidden nodes and collisions with unsaturated competing links. The first failure probability is monotonically decreasing function and the second failure probability is monotonically increasing function with respect to increase in the number of transmissions on the primary link. Thus, we increment the number of transmissions on the primary link until the first failure probability determined from DCF backoff procedure converges to the second one. The difference between this maximum allowable number of successful packet deliveries and the current level of the traffic at the primary link gives the residual

bandwidth.

4.2 Modeling Busy Period

In order to determine the utilization of channel among primary and competing links, we first study the period of time in which the primary link is busy due to the activities of the competing links. Then, the busy period is used to obtain the idle period. During calculation of busy period, we consider overlapping period of the competing links' transmission due to FIM problem.

To obtain the period, we determine the period of the transmission for each competing link. To determine the duration of successful and failed transmissions, corresponding to all transmission attempts, we first define N_i as the number of successful transmissions on competing link i. The total average number of transmission attempts on competing link i is $\frac{N_i}{1-p_i^f}$, where p_i^f is the overall packet failure probability on that link. Then, the duration of transmissions on competing link i in a unit time, $|T_i|$, can be obtained as:

$$|T_i| = \frac{N_i}{1 - p_i^f}(T_i^{tr} + D), \tag{5}$$

where T_i is interval of time occupied by transmission on competing link i in unit time, and T_i^{tr} is the mean time spent for the transmission of a packet until the reception of its acknowledgment per transmission attempt and D is distributed inter-frame space (DIFS) time. The product of $(T_i^{tr} + D)$ and the average number of transmission attempts in unit-time gives proportion of time consumed for transmission activities. Let S be the average packet payload size and $SIFS$ be the short inter-frame space. Then, the mean transmission time,

T_i^{tr}, is given as in [25],

$$
\begin{aligned}
T_i^{tr} &= T_i^{data} + SIFS + T_i^{ACK} \qquad (6)\\
T_i^{data} &= \frac{PLCP_{Preamble,i}+PLCP_{Header,i}}{Basic.Rate}+\frac{MAC_{Header,i}+FCS}{Data.Rate_i}\\
&\quad +\frac{S}{Data.Rate_i},\\
T_i^{ACK} &= \frac{PLCP_{Preamble,i}+PLCP_{Header,i}}{Basic.Rate}+\frac{ACK_{Header,i}+FCS}{Data.Rate_i}.
\end{aligned}
$$

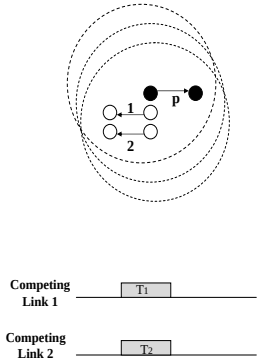

(a) Competing links 1 and 2 can sense each other

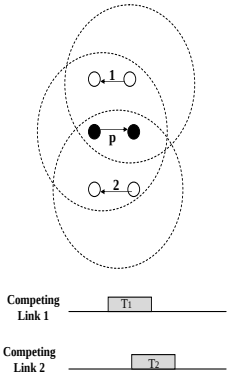

(b) Competing links 1 and 2 cannot sense each other

Figure 10: Competing Link Configurations

If all transmissions occur at distinct instants, the busy period is the sum of the average transmission time of each competing link. However, note that, some of the competing links' transmission events may overlap within them-

selves or with the primary link, hence we have to calculate and subtract such overlapped intervals from the time spent by the transmissions of the competing links. Thus, the total time the channel is busy for the primary link can be represented as:

$$T_{busy} = \sum_{i \epsilon \nu(s)} |T_i| - \left| \bigcup_{i,j \epsilon \nu(s)} T_i \cap T_j \right| - \left| \bigcup_{i \epsilon \nu(s)} T_p \cap T_i \right|, \tag{7}$$

where T_p is transmission time interval for the primary link and $\nu(s)$ denotes set of competing links originating from the neighbors of sender s of the primary link. In (7), the second term represents the union of the overlapped intervals between competing links, and the third term is the union of the overlapping intervals between the primary link and each competing link. The duration of the overlap between competing links, can be approximated as:

$$\left| \bigcup_{i,j \epsilon \nu(s)} T_i \cap T_j \right| \approx \sum_{i,j \epsilon \nu(s)} |T_i \cap T_j|. \tag{8}$$

We ignore overlap between transmissions of three or more links due to very low probability of occurrence. Note that, overlap between competing links is location dependent. Fig. 10(a) illustrates an example network, where competing links 1 and 2 can sense each other, and overlap can be seen when they begin transmissions simultaneously. Fig. 10(b) depicts how competing links 1 and 2 may not be in the sensing range of each other and overlap takes place, when a station starts to transmit while other station is already transmitting, as observed in FIM situation. Thus, we make following analysis to determine overlapping duration of the transmissions between two competing links i and j:

1. If the senders of two links cannot sense each other but have common neighbors, then transmissions over these two links cannot take place within the time used by their common neighbors. Thus, transmissions over these two links can overlap in the remaining time, which is not occupied by their

common neighbors. Then, the overlapping time of competing links i and j, $|T_i \cap T_j|$, is obtained as follows:

$$|T_i \cap T_j| = \frac{|T_i|.|T_j|}{1 - \sum_{k \in \eta(i,j)} |T_k|}, \tag{9}$$

where $\eta(i, j)$ denotes the set of links, transmissions which are sensed by both competing links i and j. $|T_k|$ is the average transmission time of a link in this set. (9) assumes that the transmissions between links that are outside of each other's sensing range are independent, and average transmission time of competing link i, $|T_i|$, gives the probability that a transmission slot in unit time interval is occupied by competing link i. Since these links do not transmit when their common neighbors use the channel, overlap can occur in the remaining time, $1 - \sum_{k \in \eta(i,j)} |T_k|$, where their common neighbors do not occupy the channel. For example, in Fig. 8(b), the common neighbor of competing link 1 and 2 is the primary link and overlapping time between these links is given as $|T_1|.|T_2|/(1 - |T_p|)$.

2. Overlap may occur between competing links, which sense their transmissions. The probability of such an overlap between competing links i and j is equal to the probability that they begin their transmissions simultaneously, which will be derived in section 4.4.1 as $p_j^c(i)$. More precisely, $p_j^c(i)$ gives the fraction in which competing links i and j's transmissions take place concurrently. Thus, the product of the transmission time of competing link i with the probability, $p_j^c(i)$, gives the duration of an overlap in unit time interval between competing link i and j:

$$|T_i \cap T_j| = |T_i|.p_j^c(i). \tag{10}$$

Clearly, the primary link can sense transmissions on the competing links and overlap can occur only when they begin their transmissions simultaneously, so the union in the third term in (8) is obtained as:

$$\left| \bigcup_{i \epsilon \nu(s)} T_p \cap T_i \right| = |T_p|(1 - \prod_{i \epsilon \nu(s)} (1 - p_i^c(s))), \tag{11}$$

where $p_i^c(s)$ is the probability that competing link i and the sender of the primary link begin their transmissions in the same slot, which is again calculated in section 4.4.1. By combining the probability, $p_i^c(s)$ for each competing link, we find the probability that the sender of the primary link begins its transmission with any of the competing links at the same time. This probability represents what fraction of the primary link's transmission overlap with the competing links.

4.3 Modeling Idle Period

In this section, we will obtain the idle portion of time for a link in saturation which is only composed of backoff times and we will show that the idle period is directly dependent on the failure probability. Thus, after determining the idle period, we will extract the failure probability.

The idle portion of time for a link in saturation is only composed of backoff times. Also, the idle period is the fraction of time remaining after considering the busy period due to transmission activities on competing links (including successful and unsuccessful transmissions on the primary link). Thus, a unit time is shared between the busy and idle periods of time as follows:

$$T_p^{idle} = 1 - |T_p| - T_{busy}, \tag{12}$$

where $|T_p|$ is average transmission time in a unit time interval over the primary link containing both successful and unsuccessful transmissions. $|T_p|$ is in turn defined as:

$$|T_p| = \frac{N_p}{1 - p_p^f}(T_p^{tr} + D). \tag{13}$$

Assuming that time is slotted with slot length being μ, let us focus on the idle backoff periods on the primary link and instantaneous transmissions. This approach is similar to the one used in the seminal work by Bianchi [14], since the contention and collision behavior of 802.11 DCF can be modeled as a discrete-time random process. Then, if $\bar{B}_p$ is the mean backoff time per attempt in the primary link, the idle time under saturation can be expressed as follows:

$$T_p^{idle} = \frac{N_p}{1 - p_p^f} \overline{B}_p. \tag{14}$$

The mean backoff time per attempt ($\overline{B}_p$) can be determined in terms of p_p^c and the minimum contention window size, W_{min}, by observing the binary exponential backoff behavior. According to 802.11 MAC, the mean backoff time increases exponentially at each re-transmission, e.g., at k^{th} re-transmission the mean backoff time is $\mu(2^k W_{min} - 1)/2$. In order to keep analytical solution compact, let us assume that there is no maximum retransmission limit. Then, the mean backoff time per packet, $\overline{B}_{total}$ is,

$$\begin{aligned} \overline{B}_{total} &= \sum_{i=0}^{\infty} (1 - p_p^f)(p_p^f)^i \left(\frac{1}{2} \sum_{k=0}^{k=i} (2^k W_{min} - 1)\mu \right), \\ &= \frac{\mu W_{min}}{2(1 - 2p_p^f)} - \frac{\mu}{2(1 - p_p^f)}. \end{aligned} \tag{15}$$

In the primary link, the average number of attempts per single successful packet delivery is $1/(1 - p_p^f)$. By using this and (15), we have

$$\begin{aligned} \overline{B}_p = \overline{B}_{total}(1 - p_p^f) &= \frac{\mu W_{min}(1 - p_p^f)}{2(1 - 2p_p^f)} - \frac{\mu}{2} \\ &\approx \frac{\mu W_{min}(1 - p_p^f)}{2(1 - 2p_p^f)}. \end{aligned} \tag{16}$$

Last equation follows from $W_{min} >> 1$ and $\frac{1-p_p^c}{1-2p_p^c} > 1$, and $\mu/2$ is much smaller than the first term. If we insert (16) into (14) we obtain,

$$p_p^f = \frac{1}{2} - \frac{\mu . W_{min} . N_p}{4 . T_p^{idle}}. \tag{17}$$

(17) gives us a fundamental relationship between the failure probability of the primary link p_p^f and N_p,which is the number of successful packet transmissions in the primary link. Note that, T_p^{idle} can be determined from (12).

4.4 Computation of Failure Probability

In this section, we compute the failure probability of the primary link by considering neighboring transmissions, hidden nodes and channel impairments. As previously mentioned, the residual bandwidth will be obtained, when the failure probability calculated in this section, converges to the failure probability calculated through backoff duration, in other words, the idle period.

We identify three different categories of failures in the primary link occurring in the MAC and physical layers:(1) Failure due to collision between neighboring stations, which occurs with probability, p_p^c. (2) Failure due to hidden nodes, which occurs with probability, p_p^h. (3) Failure due to channel impairments such as path loss, fading, shadowing etc, which is assumed to occur with average probability, p_p^e. We propose the analytical solutions to obtain failure probabilities in (1) and (2), in this work and the failure probability due to channel errors can be deduced using the method in [24]. Basically, the collision detection scheme in [24] conducts accurate collision detection in two phases, named as Failure Notification (FN) and Collision Notification (CN). In the FN phase, a station disseminates the information about a failed transmission, i.e., transmission time, and the rest of the stations judge the cause by checking the received information against their own transmission history, in which the times of failed transmissions are recorded. If a station detects a collision through the FN phase, it starts the CN phase by disseminating the collision information so that the rest of the collision-involved stations self-detect the collision. Once collisions are detected, we can obtain the failure probability due to the channel impairments by subtracting the number of col-

lisions from the total number of failed transmissions.

The losses in different categories are analyzed independently and the results are combined to obtain the overall failure probability according to the following relation:

$$p_p^f = 1 - (1 - p_p^c)(1 - p_p^h)(1 - p_p^e). \tag{18}$$

In (18), the overall failure probability calculated through the fact that a transmission is successful only when it is not subject to any type of independent failures.

4.4.1 Collisions between Neighboring Stations

Analysis in this section provides insights for the main deficiency of the existing methods on the residual bandwidth estimation. Foremost, in the previous works, collisions due to competing links' transmissions are calculated by assuming that these links are saturated, where in fact they are often unsaturated. Thus, we extend our analysis to take into account the unsaturated behavior of the competing links. In addition, some papers like e.g. [19] do not consider collisions between neighboring stations; however, as demonstrated in Section V, these collisions can affect residual bandwidth estimation significantly in typical wireless mesh scenarios.

There has been recent interest in understanding the behavior of unsaturated 802.11 links, and [25] provides an analysis using a state-transition scheme based on a finite load source model. Based on the approach in [25], we define q as the probability of having an empty MAC buffer after the last packet transmission ends. According to 802.11 DCF standard, if the MAC buffer of a node is empty, sender enters the post-backoff stage, where the system waits for a backoff time randomly chosen between $[0, W_{min} - 1]$ slots. After this post-backoff stage, MAC buffer is checked. If there is a new packet arrival, the packet is directly transmitted. Let q' be the probability of having an empty

MAC buffer after the post-backoff stage. In this case, the transmitting node enters a waiting stage with probability q'. Upon an arrival, transmitting node senses the medium. If the medium is idle (with probability p^{idle}), then packet is immediately transmitted; otherwise (with probability $1 - p^{idle}$), then the system proceeds with standard backoff.

In order to have an analytical model that does not rely on a specific packet arrival pattern or complicated queuing dynamics, two simplifications have been carried out in the above model. First, the waiting time after post-backoff is neglected, and we assume that a new packet arrives just after the second MAC buffer check. Omission of waiting time in waiting state makes mathematical analysis less complicated and less dependent on packet arrival statistics like inter-arrival times. Second, we assume that $q' \simeq q$. This is a valid assumption, since the mean post-backoff time is significantly smaller than the mean packet inter-arrival time for a great majority of traffic arrival patterns.

The probability of having an empty MAC buffer in the sender of competing link i, q_i, can be approximately determined by using Little's theorem as:

$$q_i = 1 - \lambda_i E[ST_i], \tag{19}$$

where λ_i is the average packet arrival rate and $E[ST_i]$ is the expected service time on competing link i. We can identify four different states under which $E[ST_i]$ needs to be calculated. Also we define $B_{l,i}$, $B_{lpb,i}$, and F_i as the mean backoff, post backoff and backoff freeze durations per successful delivery for competing link i, respectively. $P(k)_i$, $k = 1, \ldots, 4$ denotes the probability of occurrence of each of the states, and $\overline{ST}_{k,i}$ denotes the average service for each state. These states are described as follows:

- State 1 indicates non-empty buffer after transmission with $\overline{ST}_{1,i} = B_{l,i} + F_i + T_i^{tr}$ and $P(1)_i = 1 - q_i$.

- State 2 indicates non-empty buffer after post-backoff stage with $\overline{ST}_{2,i} =$

$B_{lpb,i} + F_i + T_i^{tr}$ and $P(2)_i = q_i(1 - q_i)$.

- State 3 indicates empty buffer after post-backoff, channel busy with $\overline{ST}_{3,i} = \frac{1}{\lambda_i} + B_{l,i} + F_i + T_i^{tr}$ and $P(3)_i = q_i^2(1 - p_i^{idle})$.

- State 4 indicates empty buffer after post-backoff, channel idle, transmit directly; $\overline{ST}_{4,i} = \frac{1}{\lambda_i} + F_i + T_i^{tr}$ and $P(4)_i = q_i^2 p_i^{idle}$.

Thus, the average service time for competing link i, $E[ST_i]$, considering all states, is calculated as,

$$E[ST_i]=(1-q_i)\overline{ST}_{1,i}+q_i(1-q_i)\overline{ST}_{2,i}+q_i^2(1-p_i^{idle})\overline{ST}_{3,i}+q_i^2 p_i^{idle}\overline{ST}_{4,i}. \quad (20)$$

Note that, the proportion of time channel is idle per unit time interval as seen by competing link i is simply the union of transmission time of its neighbors and it is given as:

$$p_i^{idle} = 1 - \left| \bigcup_{j \epsilon \nu(i)} T_j \right|, \quad (21)$$

where $\nu(i)$ denotes the set of neighbors of competing link i. The idle time is the remaining period in a unit interval when the transmissions over the neighboring links of competing link i are deducted. Backoff freeze occurs in a unit interval at competing links when there is another ongoing transmission on the channel. The total proportion of time where backoff freeze occurs in competing link i during state 1, B_i^{fr}, is calculated following the same analysis as in section 4.2,

$$B_i^{fr} = (1 - q_i) \left| \bigcup_{j \epsilon \nu(i)} T_j \right|. \quad (22)$$

Fig. 11 depicts an example network where all senders except for the sender of competing link 1 can hear each others transmission. The sender of competing link 1 can only hear transmissions on the primary link and there exists a hidden node, which can be sensed by links 2 and 3. In this example, competing

link 2 hears the transmissions on the primary link, competing link 3 and the hidden link, but the sender of the primary link and the hidden link cannot sense each other's transmissions. Thus, idle probability for competing link 2 is $1-(|T_3|+|T_p|+|T_h|-|T_p \cap T_h|)$, where T_h is the average transmission time of hidden link h and $|T_p \cap T_h|$ is the overlapping period between the primary link and the hidden link.

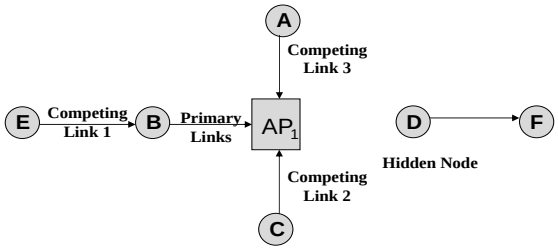

Figure 11: Typical network scenario with hidden node

Note that, F_i is the ratio of B_i^{fr} to the number of successful packet deliveries in unit time, i.e., $\frac{B_i^{fr}}{N_i}$. Meanwhile, the mean backoff and mean post-backoff times for competing links can be determined similar to $\overline{B_p}$, as:

$$\begin{aligned} \overline{B}_{l,i} &= \frac{\mu W_{min}(1-p_i^f)}{2(1-2p_i^f)} \\ \overline{B}_{lpb,i} &= \frac{\mu(W_{min}-1)}{2}(1-p_i^f)+p_i^f\overline{B}_{l,i}. \end{aligned}$$

After appropriate simplifications, we insert (20) into (19), we obtain the following quadratic equation for q_i in terms of λ_i, F_i , p_i^{idle}, $\overline{B}_{l,i}$, $\overline{B}_{lpb,i}$ and T_i^{tr}.

$$\begin{aligned} [\lambda_i\overline{B}_{l,i}(1-P_i^{idle})+1-\lambda_i\overline{B}_{lpb,i}]q_i^2+[\lambda_i(\overline{B}_{lpb,i}-\overline{B}_{l,i})+1]q_i+ \\ \lambda_i(\overline{B}_{l,i}+F_i+T_i^{tr})-1=0. \end{aligned} \tag{23}$$

Since λ_i is the average packet arrival rate for any of the competing links, we simply have $\lambda_i = N_i$. Therefore, all the coefficients in (23) can be written in terms of N_p, p_i^f, p_p^f and the measured variable, N_i.

A transmission in a competing link can only take place when there are no transmissions in the primary link and its common neighboring links with the primary link. Similarly, a transmission in the primary link can only occur if the competing link and its common neighbors are idle. Thus, transmission probability of a competing link i observed by the primary link is:

$$p_i^t(s) = \frac{\mu.N_i}{(1-p_i^f)} \times \frac{1}{1-|T_p|-|T_i|-\sum_{k\epsilon\eta(s,i)}|T_k|}. \tag{24}$$

The collision probability of the primary link, p_p^c, should be calculated by taking into account that the competing links are unsaturated. Note that, p_p^c can be written as the probability of observing a transmission in at least one of the competing links, given that a transmission is already occurring on the primary link. Due to the special transmission behavior of unsaturated links (transmit directly after sensing idle instead of transmitting after backoff), for every competing link i unit backoff time is separated into two disjoint regions corresponding to different pair-wise collision behavior between the primary and the competing link i. By using the definition of transmission probability in (24), probability that the competing link i transmits after backoff/post-backoff is

$$p_{backoff,i}^t = (1-P(4)_i)p_i^t(s), \tag{25}$$

and the probability that competing link i transmits directly is

$$p_{direct,i}^t = P(4)_i p_i^t(s), \tag{26}$$

where $P(4)_i = q_i^2.P_i^{idle}$. Thus, the pair-wise collision probability between the primary link and competing link i is obtained as follows,

$$p_i^c(s) = (p_{backoff,i}^t(1-P(4)_i)) + p_{direct,i}^t P(4)_i. \tag{27}$$

Finally, p_p^c is derived from pair-wise collision probabilities as

$$p_p^c = 1 - \prod_{i\epsilon\nu(s)\cup i\epsilon\nu(s')} (1-p_i^c(s)). \tag{28}$$

Here, s' denotes the receiver of the primary link. Transmissions of neighboring stations may cause collision only when its transmissions are sensed by the receiver of the primary link. Transmissions over the competing links may also collide with the transmissions on the primary link and other competing links. The transmission probability of the primary link with respect to the competing link i is similarly found as:

$$p_p^t(i) = \frac{\mu.N_p}{(1-p_p^f)} \times \frac{1}{1-|T_p|-|T_i|-\sum_{k\epsilon\eta(s,i)}|T_k|}. \tag{29}$$

Due to saturation assumption of the primary link, the sender of the primary link always has a packet in its queue. Thus, the collision probability of the competing link i with the primary link is equal to $p_p^t(i)$. To find the collision probability between the competing links, we first find their transmission probabilities with respect to each other as:

$$p_j^t(i) = \frac{\mu.N_i}{(1-p_i^f)} \times \frac{1}{1-|T_j|-|T_i|-\sum_{k\epsilon\eta(i,j)}|T_k|}. \tag{30}$$

Then, the collision probabilities of these links are calculated in a similar fashion as we have done to calculate the collision probability of the primary link. Thus, we obtain the collision probability between competing links i and j as:

$$p_j^c(i) = ((1-P(4)_i)p_i^t(j))(1-P(4)_i) + (P(4)_i p_i^t(j))P(4)_i. \tag{31}$$

Overall, the failure probability of the competing link i is:

$$p_i^f = 1-(1-p_i^{fn})(1-p_p^t(i)) \prod_{j\epsilon\nu(i)\cup j\epsilon\nu(i')} (1-p_j^c(i)), \tag{32}$$

where the index i' denotes the receiver of the competing link i.

4.4.2 Failures due to Hidden Nodes

The impact of hidden nodes on the performance of wireless multi-hop networks is crucial. We analyze hidden node problem not only by considering DATA-DATA collisions but also considering DATA-ACK collisions. In this respect,

we consider the hidden node problem in two cases according to location of hidden node with respect to the primary link, as shown in Fig. 12. Each of these cases yields a different solution for the failure probability.

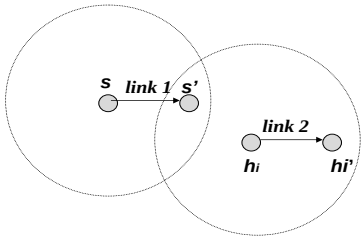

(a) Case 1: DATA-DATA collision with hidden link

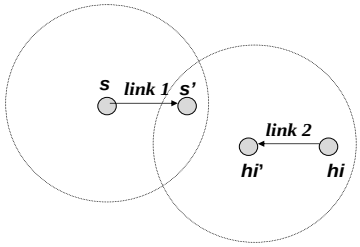

(b) Case 2: DATA-ACK collision with hidden link

Figure 12: Hidden Node Configurations

Case 1: Let link 1 be primary link, where s is the sender of link and s' is the receiver. In the same sense, let link 2 be the link containing hidden node for link 1. If R_s is the sensing range and $r(x, y)$ denotes the distance between nodes x and y, then case 1 occurs when the following configurations take place:

1.$r(s, h_i) > R_s$, i.e. senders are not in the sensing range,

2.$r(s, h_i') > R_s$, i.e. receiver of the hidden link is not in the range of the sender of the primary link,

3.$r(s', h_i) < R_s$, i.e. sender of the hidden link is in the range of the receiver of the primary link,

4.$r(s', h_i') > R_s$, i.e. receiver of the hidden link is not in the range of the

receiver of the primary link.

Let N_{h_i} be the number of successful data transmissions by hidden link i. The total average number of transmission attempts in unit time interval on hidden link i is $\frac{N_{h_i}}{1-p_i^f}$, where $p_{h_i}^f$ is the overall packet failure probability on that link. If hidden node and sender of the primary link have common neighbors, then their transmissions can only overlap and result in collision during the period in which there is no transmission on the common links. Hence, the time in which collision may occur is $1 - \sum_{k\epsilon\eta(h_i,s)} T_k$, and given there are $1/\mu$ slots in a unit time interval, the transmission probability of the sender of hidden link i in a slot, $p_{h,i}^t(s)$ is given as:

$$p_{h,i}^t(s) = \frac{N_{h_i}.\mu}{1 - P_{h_i}^f} \times \frac{1}{1 - \sum_{k\epsilon\eta(h_i,s)} |T_k|}. \tag{33}$$

Here, $\eta(h_i, s)$ represents common neighbors of the primary link and hidden link i. To illustrate (34), we again use the example in Fig. 9. In Fig. 9, the hidden link and the primary link have competing links 2 and 3 as common neighbors. Their transmissions cannot overlap when the channel is occupied by the transmissions on competing links 2 and 3, so the time in which collisions may occur, is $1 - |T_2| - |T_3|$.

In this case, collisions occur during the time when there is a transmission on the primary link and the hidden link starts transmitting. The receiver node of hidden link does not hear the transmission on the primary link. Thus, only the primary link suffers from collisions, and the collision probability in the primary link due to transmissions of hidden link i is computed as follows

$$p_{p,i}^h(s) = \left[1 - (1 - p_{h,i}^t(s))^m\right], \tag{34}$$

where m is the number transmission opportunities of the hidden link i. Note that, m is equal to $\lfloor \tau/\mu \rfloor$, where τ is the total duration of the packet and ACK sent on the primary link and the packet sent on the hidden link.

Case 2: The configuration in case 2 is as follows:

1.$r(s, h_i) > R_s$, i.e., senders are not in the sensing range,

2.$r(s, h'_i) > R_s$, i.e., receiver of the hidden link is not in the range of the sender of the primary link,

3.$r(s', h_i) > R_s$, i.e., sender of the hidden link is not in the range of the receiver of the primary link,

4.$r(s', h'_i) < R_s$, i.e., receiver of the hidden link is in the range of the receiver of the primary link.

In this case, two links are connected only through their respective receivers, and a collision occurs whenever the control packet sent by one receiver interferes with the reception of the DATA packet at the other receivers. This time, we use the number of ACK transmission attempts from the receiver of the hidden link i as h'_i, instead of DATA transmission attempts. The transmission probability of the receiver of hidden link i is written as:

$$p^t_{h,i'}(s) = \frac{N_{h'_i}.\mu}{1 - \sum_{k \epsilon \eta(h_i,s)} |T_k|}. \tag{35}$$

The collision probability is obtained from (34) similar to case 1. However, m, the number of transmit opportunities is calculated from τ considering the duration of DATA and ACK sent in the primary link in addition to ACK sent by the receiver of the hidden link in terms of number of time slots.

After computing the collision probability for each hidden link, the total collision probability due to hidden node for the primary link is calculated as:

$$p^h_p = 1 - \prod_{i \in \kappa(s)} (1 - p^h_{p,i}(s)), \tag{36}$$

where $\kappa(s)$ is the set of hidden links for the primary link.

Fig. 13 depicts the flow chart of our residual bandwidth estimation algorithm, illustrating the combination, iteration of the steps and calculations of the analysis described so far. In the algorithm, we first obtain the busy period and the idle period for each N_p and then we extract the first failure probability obtained from the idle period. In the meantime, we find the second failure

probability by combining collisions with competing links, collisions due to hidden nodes and the loss probability due to fading. If the first and the second failure probabilities converge to the same value, then we obtain the residual bandwidth in terms of the number of packets, N_p. Otherwise, we increase N_P and continue algorithm until both failure probabilities have the same value.

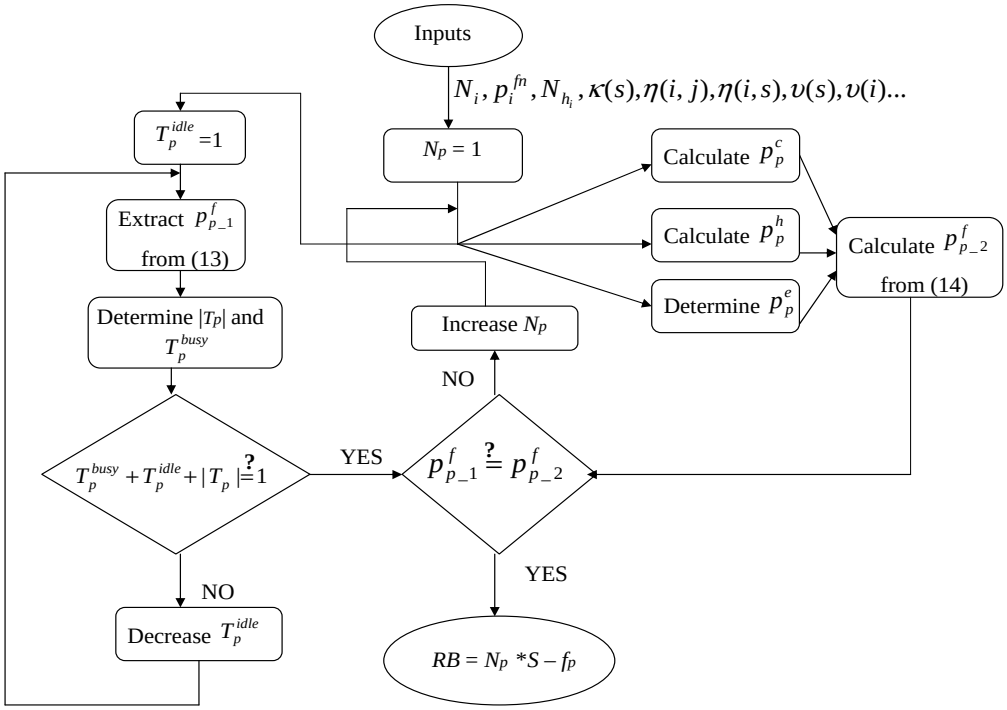

Figure 13: Flow Chart that summarizes our RBW estimation algorithm

5 SIMULATION ENVIRONMENT

OPNET Modeler is a network simulation software that allows us to design and study communication networks, devices, protocols, and applications [26]. It provides a graphical editor interface to build models for various network entities from physical layer modulator to application processes.

5.1 Network Modeling with OPNET

OPNET has ability to simulate a wide range of communication systems from a single LAN to a global satellite network. By modeling a network, OPNET uses a hierarchical system in which higher levels utilizes models developed in lower levels. By doing that, different generic models can be used under many different scenarios and modifications can be easily made by only changing the models.

OPNET uses a project and scenario approach to model networks. Project is a collection of related network scenarios in which each explores a different aspect of network design. A project contains at least one scenario and a scenario is a single instance of a network containing all the information. It is possible to run all the scenarios of the network at the same time and compare the results of each one.

5.2 IEEE 802.11 Node Models

Node models are objects in a network model. They are made up of modules with process models, which control module behavior and may reference parameter models. The Node Editor lets you define the behavior of each network object. The Fig. 14 shows the WLAN Node Models, where important modules for our algorithm are "*wireless_lan_mac*", which contains wlan process model and "*manet_rte_mgr*", where routing protocols are implemented. "*traf_src*"

create raw packets with specified size and rate.

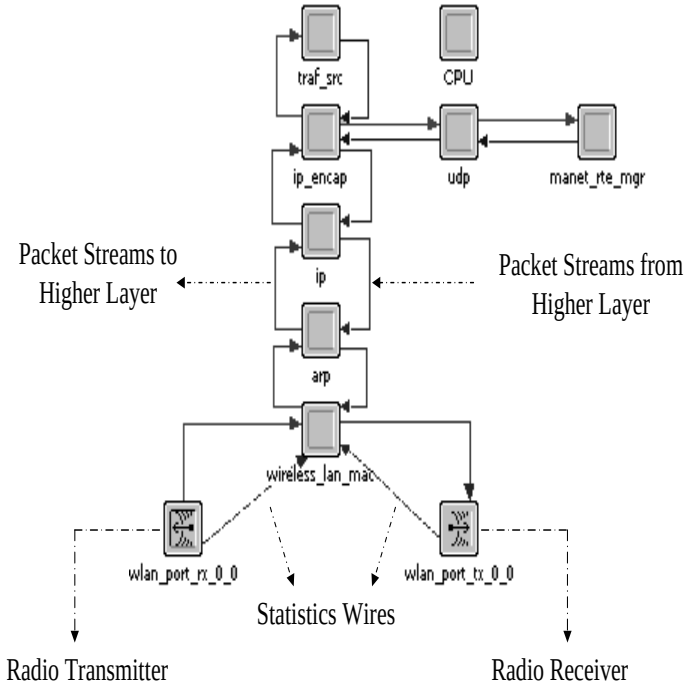

Figure 14: WLAN Node Model

5.3 IEEE 802.11 Process Model

The MAC process model stores the main code of our model. The statistics of one and two hops away nodes are collected in this section and they inserted in our algorithm to find the residual bandwidth. There are two types of interrupts; the stream interrupts occur at either higher layer data arrival and lower physical layer data arrival. The lower layer data arrival interrupt invokes the "*wlan_physical_layer_data_arrival*" function and we collect the necessary statistics, like the number of competing links and the number of transmissions on these links, the number of hidden nodes, etc.

The process model consists of many states. It makes transitions between these states according to appropriate interrupts and executes the defined functions during the transitions or in the states. In $INIT$ and BSS_INT, all variables like MAC auto-addresses or state variables are initialized. In $IDLE$ state, MAC buffer of the station is empty, and wait for a higher layer data arrival interrupt. $DEFER$ state carries out deferring due to transmission on the neighboring links and update NAV. In $BKOFF\_NEEDED$ and $BACKOFF$ states, it is decided whether backoff is necessary or not and if it is necessary, then it chooses the backoff slots during which the backoff counting is realized. $TRANSMIT$ state realizes the packet transmission. FRM_END and $WAIT\_FOR\_RESPONSE$ states decide whether the transmission is successful or collision is occurred.

5.4 Channel Model

The wireless channel in OPNET modeler is modeled in different pipeline stages, which compute propagation delay, antenna gains, signal-to-noise ratio, transmission delay, etc. The path loss, which is signal attenuation related with distance between transmitter and receiver, represents the difference between transmitted signal power and the received signal power. OPNET assumes the free space propagation model for the path loss, PL, in other words,

$$PL = \frac{\lambda^2}{16\pi^2 d^2}, \tag{37}$$

where λ is the wavelength in meters and d is the distance between transmitter and receiver antenna. The average received power is calculated as follows:

$$\bar{P_r} = P_t * tx\_ant\_gain * PL * rx\_ant\_gain, \tag{38}$$

where P_t is transmit power, and tx_ant_gain and rx_ant_gain are respectively transmitter antenna gain and receiver antenna gain. We modify the pipeline

stage and add rayleigh fading as a multi-path fading. As known, the power of a signal, P_r, that is perturbed by Rayleigh type of fading is exponentially distributed with average received power calculated in (38) as the mean. Thus, the probability density function of received power is as follows:

$$f(P_r, \bar{P}_r) = \frac{1}{\bar{P}_r} e^{\frac{P_r}{\bar{P}_r}}. \tag{39}$$

As noise sources, OPNET considers both background and thermal sources that are summed as the background noise, in addition to interfering packets. When receiver temperature and background temperature are known, then the background noise is calculated as follows:

$$N = k * T * B, \tag{40}$$

where k is the Boltzmann's constant, T is the sum of receiver temperature and background temperature and B is receiver channel bandwidth (in Hz).

Signal to interference plus noise ratio (SINR) is calculated by considering both the background noise and interfering packets as:

$$SINR = \frac{P_r}{\sum_{j=1}^{n} I_j + N}, \tag{41}$$

where I_j represents j^{th} interfering packet and there are total n interfering packets.

6 PERFORMANCE ANALYSIS

In this section, we validate the strengths of our estimation algorithm by first evaluating its accuracy against the most recent scheme [19] and two most prominent passive methods, and then, we present our results on improved advanced network services, where residual bandwidth estimation is implemented into admission control and intelligent routing. We present simulation results, that are obtained from a detailed wireless mesh network model with IEEE 802.11g based air interface and MAC, devised in OPNET environment. Table 2 shows the system parameters that are used in the simulation.

Table 2: Simulation Parameters

Transmission range	200m
Carrier-Sensing range	400m
Propagation model	Free Space
RTS\CTS	Disabled
Packet arrival distribution	Poisson
Packet Size	2048,4096,8192 bits
Channel rate	11,24,36,48,54 Mbps
Slot time	20 μs
SIFS	10 μs
DIFS	50 μs
CW_{min}	16
CW_{max}	1024
Routing protocol	AODV
Network area	1500mx1500m

6.1 Accuracy of the Residual Bandwidth Estimation

This section presents the simulations carried out to observe the accuracy of our algorithm in comparison to the method in [19] and two passive methods [7, 8], which propose analytical model of 802.11 DCF and estimate the end-to-end throughput capacity. To calculate the capacity, the method in [19] derives the channel idle probability by considering neighboring contention, which results in busy period and hidden node contention. Although [19] is one of the few works that calculates end-to-end throughput for the multi-hop wireless networks, this method does not consider collisions between neighboring stations and packet loss due to fading. To make a fair comparison with this algorithm and passive methods, we assume perfect channel with no fading in our model as well.

We consider three different scenarios, as depicted in Fig. 15, for performance comparison of the methods. These simple scenarios are selected such that they reflect the behavior of the wireless mesh networks and the distinctive features of our algorithm. The first scenario is a star topology, in which nodes gather around access point 1 (AP_1) and some of the flows are destined to access point 2 (AP_2), in which AP_1 forwards them to AP_2. In the second scenario, a typical multi-hop wireless network is illustrated, where the load of the competing links that are on the path with the primary link, is equal to the sum of the number of successful packet transmissions on the primary link and the other transmissions originated from the competing link or from any other link but passing through the competing link. The third scenario is selected to emphasize one of the weaknesses of the method in [19], in which the collisions with the receiver of hidden link are not considered. The load, data size and physical data rate of the links in these scenarios are selected randomly within the range of value defined in Table 2. Our results reflect the averages computed over five realizations of each scenario. As a benchmark, we also depict the actual residual bandwidth measured in the simulations, as the

simulated result.

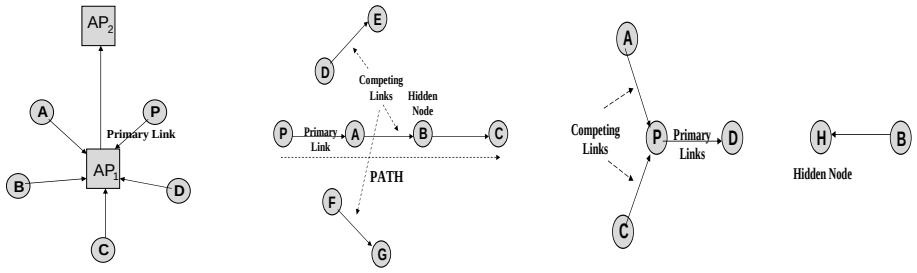

(a) Scenario 1 (b) Scenario 2 (c) Scenario 3

Figure 15: Network Scenarios

As it can be seen from the results illustrated in Fig. 16 containing the results for scenario 1, in Fig. 17 containing the results for scenario 2, in Fig. 18 containing the results for scenario 3, our computed residual bandwidth is well matched with the simulated actual value and significantly outperforms the passive methods and the method in [19]. The passive listen and time difference methods perform the worst, because they do not model backoff and collisions. Our method is shown to provide an error margin which is as low as an order of magnitude of the error observed by methods in [7] and [8]. The reason why the algorithm in [19] has relatively bad performance is that it does not consider collisions between the neighbors and the hidden node case in which the receiver of the hidden link leads to collision in primary link. However, both types of collisions have great impact on the performance of the network. For example, in scenario 1, which is typical WMN topology, the probability of such collisions is around 17%. Clearly, as the total load in the network increases, collision probabilities grow accordingly, the performance of the method in [19] is further degraded, while our method provides accurate estimation with bounded and negligibly low error margin of 1.5%. In addition, the passive methods and the method in [19] overestimate the residual bandwidth, but the estimation

of our method is more scenario dependant. For example, in scenario 2 and 3, our method overestimates the residual bandwidth, but in scenario 1, it underestimates the residual bandwidth for high loads of the competing links. Nevertheless, our estimation error is significantly lower.

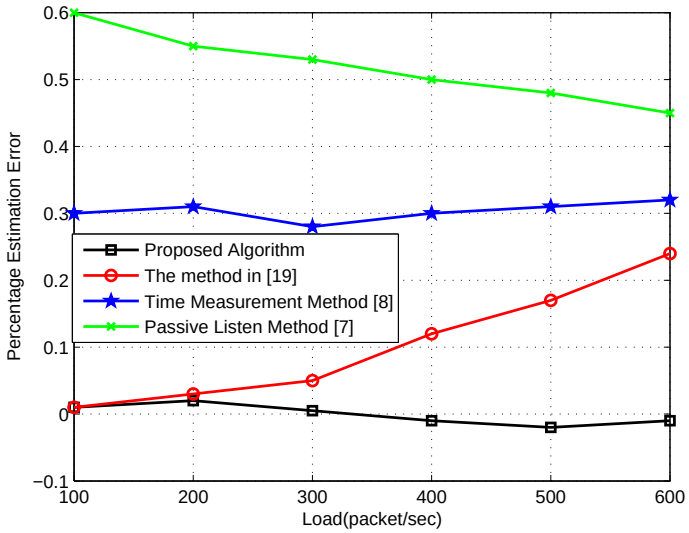

Figure 16: The Results of Residual Bandwidth Estimations—Scenario 1

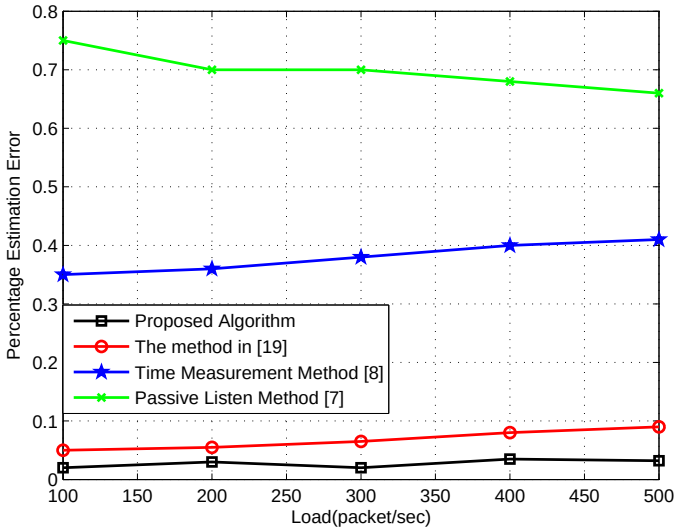

Figure 17: The Results of Residual Bandwidth Estimations—Scenario 2

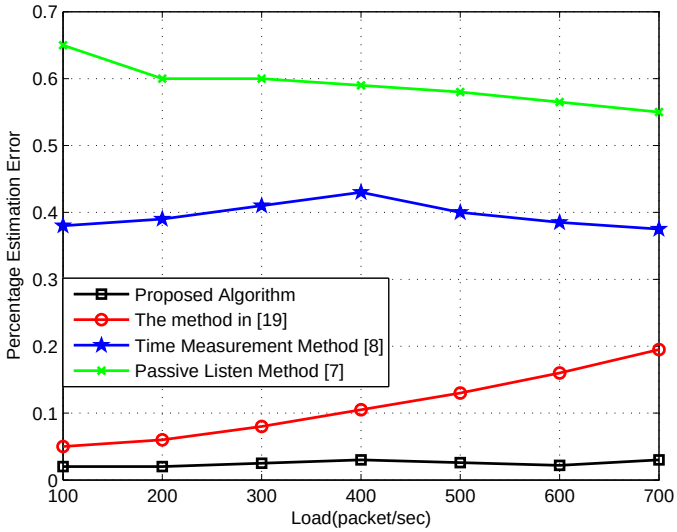

Figure 18: The Results of Residual Bandwidth Estimations—Scenario 3

We measure the performance of methods for variable loads of the competing links. The loads of competing links change over time and the load values are randomly selected. We make the simulation for scenario 1 and the update time for each method is one second. As seen in Fig. 19, maximum estimation error of our method is around 30%, but the passive methods result in up to 90% maximum estimation error and the method in [19]'s is around 45%.

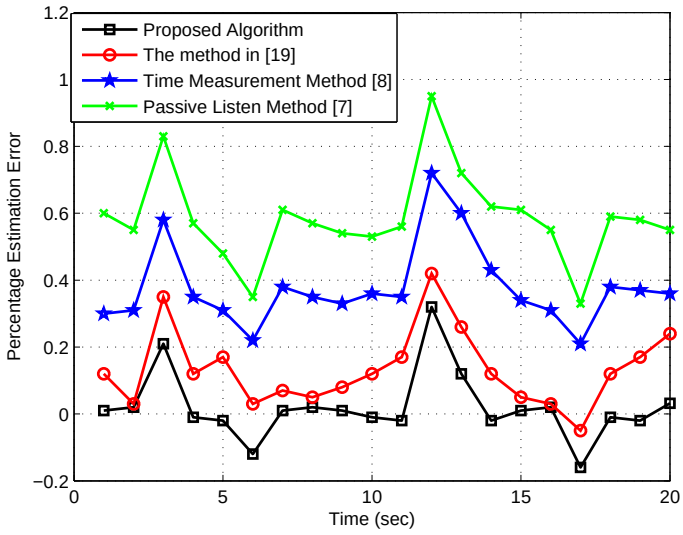

Figure 19: The Results of Residual Bandwidth Estimations for variable load

6.2 Convergence and Complexity Analysis

An important limitation of the passive residual bandwidth estimation methods is low convergence rate since they require measurement of network activity for some operational time [27]. Our proposed residual bandwidth estimation method also has the same limitation as it utilizes a network monitoring scheme that measures the activity of the competing links for an update period. In order to observe how quickly each estimation scheme responds to changes in the available network capacity, we have performed simulations on Scenario 1

depicted in Fig. 15, and we observed the estimation error as the update period is varied from 0.01 seconds to 1 second.

In Fig. 20, the convergence performance of our estimation method and passive methods are depicted. Here, we use normalized estimation error that is calculated as the absolute difference between the estimated and actual residual bandwidth values, normalized to the actual residual bandwidth. The competing links' traffic load, packet size and data rates are randomly chosen from Table 2. As shown by Fig. 20, our proposed residual bandwidth estimation method exhibits a stable performance with decreasing estimation errors as the update period is increased. The proposed method outperforms the two prominent passive methods significantly, with estimation error margin less than 1%, which is an order of magnitude of the passive listen method, and time measurement method.

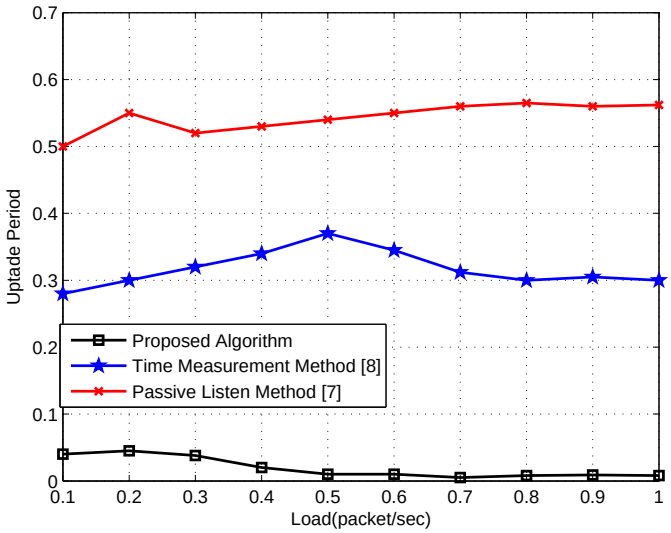

Figure 20: Convergence Analysis

Complexity of analytical models is an important parameter to the evaluation of the algorithms. In this part, we compare complexity of our proposed

algorithm and the method in [19]. In our algorithm, we increase the number of packets, N_p, on the primary link, and solve the equations for idle period, T_{idle}^p and q, which is the probability of having an empty queue. These equations are non-linear, and we have to make search for each N_p to find T_{idle}^p and q. We define Δ as the step size used during search algorithm. T_{idle}^p is obtained through one search and q is found through L, the number of neighboring links, searches. In addition, there are maximum $1/\Delta$ iterations for each search. If we blindly search for each value, then the complexity of algorithm becomes $O(N_p * (1/\Delta + L/\Delta)) \approx O(N_p * L/\Delta)$, which represents relatively high complexity for residual bandwidth estimation algorithms in large networks. By making use of shape of error functions, which are the difference between the given value and calculated value during the search, we can reduce the complexity of the proposed algorithm. The error functions are monotonically increasing functions as illustrated in Fig. 21. By using gradient optimization method, in which the next value of variable is selected according to gradient value of previous value as seen in Fig. 21, the complexity of each search can be reduced to $O(log(1/\Delta))$ instead of $O(1/\Delta)$. In addition, the search is ended when the value of error reaches to zero. Then, the complexity of our proposed algorithm becomes $O(L * (logNp) * (log(1/\Delta)))$.

The analysis in [19] is much simpler than the analysis in our algorithm, since in [19], the residual bandwidth is calculated through one non-linear equation that requires one search. For that reason, the complexity in [19] is simply $O(1/\Delta)$.

We make ten runs for the scenarios in Fig. 15 and we observe the number of mathematical operations, which are utilized to obtain the residual bandwidth. For each scenario, the number of mathematical operations except divisions for our proposed method is much lower than the one for the method in [19] as seen in Table 3. In addition, each mathematical operation requires one flop [28],

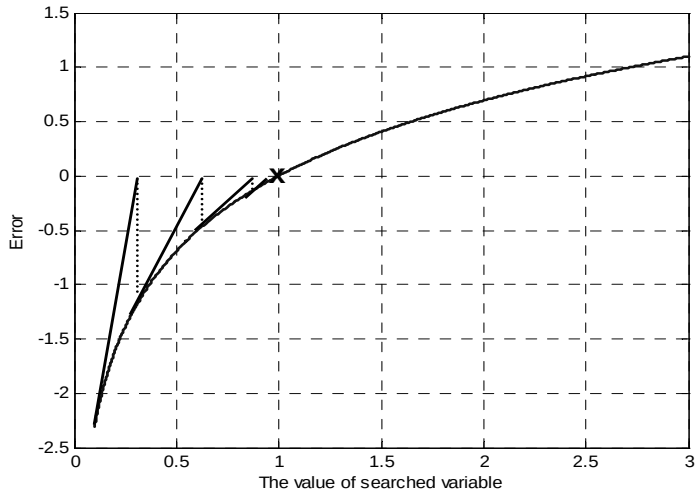

Figure 21: The error function and illustration of the gradient method

and in terms of flop counts, our algorithm outperforms the method in [19]. Our proposed algorithm uses three or four times less flops than the method in [19].

Table 3: The number of mathematical operations

	Scenario1		Scenario2		Scenario3	
	Gao	Proposed	Gao	Proposed	Gao	Proposed
Number of $+$	6600	896	8556	1792	5052	1314
Number of $-$	2200	1648	2852	3321	1684	2122
Number of $\times$	23100	2832	29946	5826	17682	4176
Number of $\div$	1100	1152	1426	2414	842	1558
Number of iterations	550	72	713	146	421	104
Number of flop counts	33000	6528	42780	13353	25260	9170

6.3 Admission Control

Here, we demonstrate the application of our residual bandwidth estimation method for flow admission control in a WMN. This time we consider a large network where 50 nodes are randomly placed in a 1500 m x 1500 m area around an access point (AP). In this setting, 10 source/destination node pairs are randomly selected out of 50 nodes, constituting 10 different end-to-end paths. One of these paths is randomly chosen as our primary path on which we apply flow control by using our residual bandwidth estimation method and [19]. The source nodes in the remaining nine paths constitute the competing flows by sending a predetermined level of traffic to their destination nodes over this WMN. We again assume perfect channel to make fair comparison with [19] and the packet arrival distribution is poisson.

For flow control purposes, the standard Ad Hoc On demand Distance Vector (AODV) protocol is modified so that the residual path bandwidth can be computed from link residual bandwidth estimates along the primary path. Residual bandwidth values estimated in the sender node of each link on the primary path are embedded in the AODV route reply messages and relayed back to the source node. The source node of the primary path calculates end-to-end path residual bandwidth by picking up the minimum of the received link residual bandwidth values. Flow admission control is then carried out such that the flow is admitted as long as the flow is smaller than minimum residual bandwidth. The simulations are performed for ten realizations of the described scenario. Fig. 22 shows the performance of the flow control scheme utilizing the residual bandwidth estimation method proposed in this work and the passive methods and Fig. 23 illustrates the result for the method in [19].

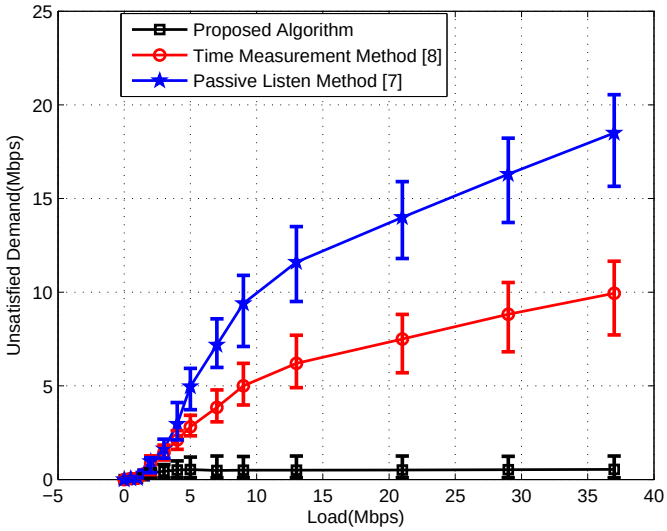

Figure 22: Unsatisfied Demand—Comparison with the passive methods

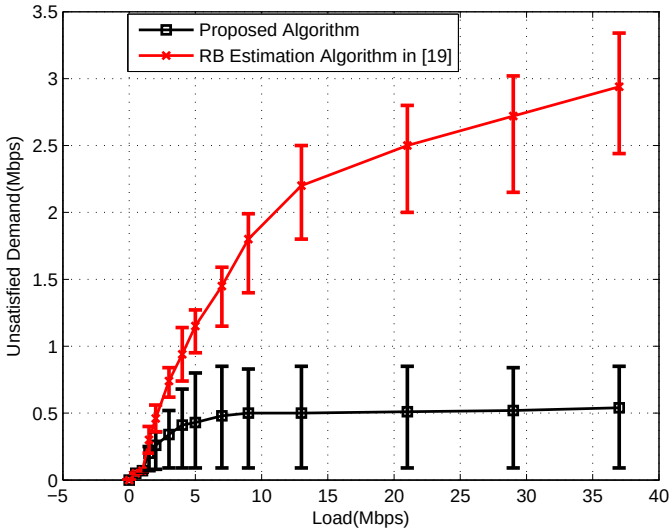

Figure 23: Unsatisfied Demand— Comparison with the method in [19]

The curves for unsatisfied traffic demand denote the average rate of traffic lost (in Mbps) due to buffer overflows in the primary path. The buffer size is assumed to be 256000 bits. The error bars in the figure indicate the maximum and minimum levels of around average unsatisfied demand observed for each method. As seen in the Fig. 22 and Fig. 23, the performance of the methods in flow admission control shows parallelism with the accuracy of the algorithms, so the passive listen method performs the worst and the time difference method is slightly better, but unsatisfied demand in this method is still large compared to analytical models,i.e., its unsatisfied demand is 20 times larger than our proposed method. With our proposed estimation algorithm, the unsatisfied demand is kept bounded and is significantly lower than the observed loss when [19] is employed. Specifically, the rate of lost or unserved traffic in [19] grows much faster and up to six times as large as our scheme. This is because, the method in [19] overestimates the residual bandwidth of the links in most cases, so flow control allows more traffic than the network can handle.

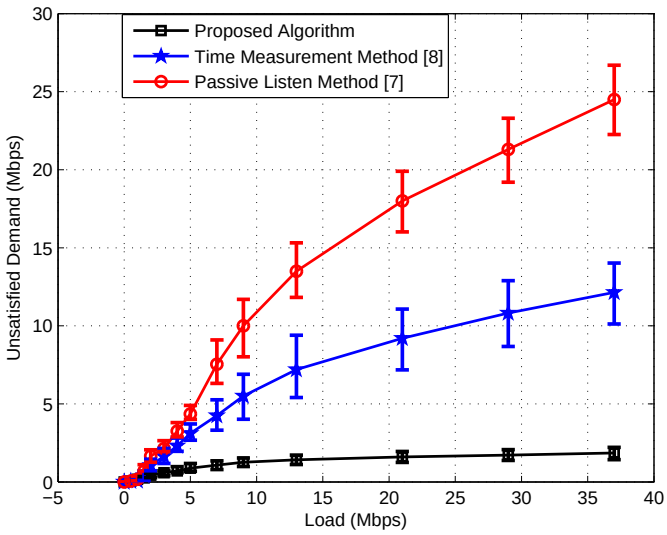

Figure 24: Unsatisfied Demand (FTP)—Comparison with the passive methods

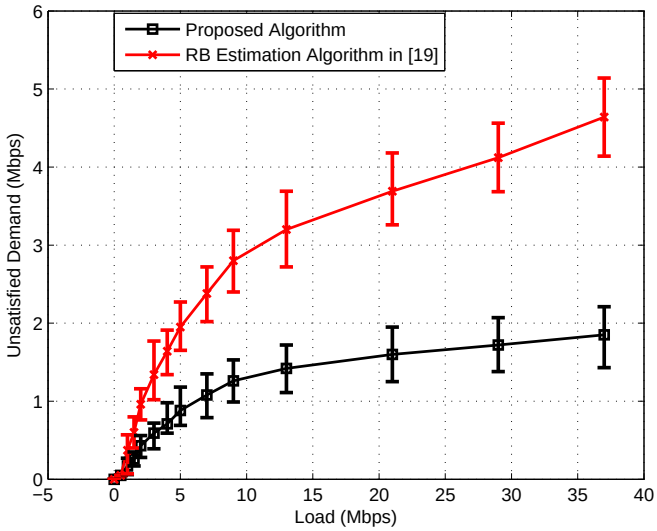

Figure 25: Unsatisfied Demand (FTP)— Comparison with the method in [19]

We also carried out the same simulation for FTP flows. As seen from Fig. 24 and 25, we get the similar results. The passive methods again has the worst performance and the admission control, which uses our proposed residual bandwidth estimation, has the lowest unsatisfied demand.

6.4 Routing

In this section, we want to observe the efficiency of a routing algorithm, which utilizes our residual bandwidth estimate. Our routing algorithm is based on well-known max-min routing [29]. More specifically, the path which has the maximum residual bandwidth is selected and the path residual bandwidth is defined as the minimum of the residual bandwidth of the links on the path.

First, we will illustrate in what degree our routing algorithm approaches to the optimal routing. In order to compare min-max routing algorithm using our residual bandwidth estimate with optimal routing, we use example network scenarios in Fig. 26. In these scenarios, there are three sources and two

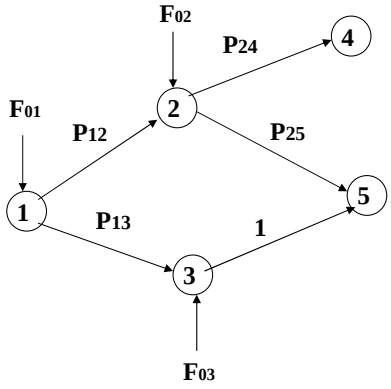

(a) Scenario 1

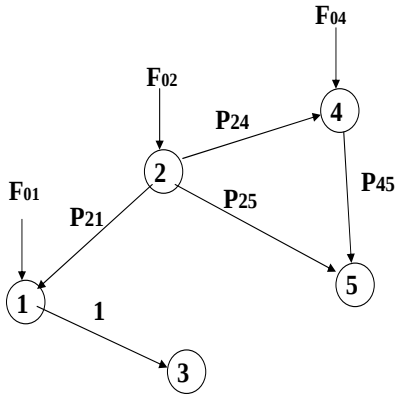

(b) Scenario 2

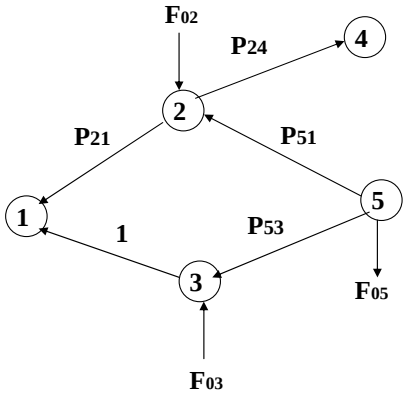

(c) Scenario 3

Figure 26: Example network scenarios for comparison of min-max routing with optimal routing

destinations and we aim to obtain load distributions in terms of the probabilities shown in the figure. The physical rate of each link is different and chosen randomly from Table 2 and each load originated from the sources is 1 Mbps. These loads are divided into chunks of 50 kbps and then routed to the destinations. The load distributions and queuing delay per node, when we use optimal routing and min-max routing algorithm, are shown in Table 4.

Table 4: The Routing Results

	Routing Type	P_{12}	P_{13}	P_{24}	P_{25}	Delay
Scenario 1	Optimal routing	0.42	0.58	0.36	0.64	0.231s
	Min-Max Routing	0.35	0.65	0.30	0.70	0.245s
	Routing Type	P_{21}	P_{24}	P_{25}	P_{45}	Delay
Scenario 2	Optimal routing	0.22	0.48	0.30	1	0.312s
	Min-Max Routing	0.20	0.55	0.25	1	0.321s
	Routing Type	P_{21}	P_{24}	P_{51}	P_{53}	Delay
Scenario 3	Optimal routing	0.38	0.62	0.56	0.44	0.198s
	Min-Max Routing	0.45	0.55	0.5	0.5	0.210s

As seen from the Table 4, optimal routing and min-max routing obtain similar results. If we consider the complexity of optimal routing as emphasized in section III, min-max routing algorithm is more applicable to practical scenarios. The other advantage of min-max routing is being distributed, in which the information about all transmission activities in the network is not needed.

In the next step, we observe how our residual bandwidth estimation method with min-max routing algorithm can contribute to the end-to-end network throughput when it is used as a routing metric. We compare our results with the popular routing metrics based on hop count and the air-time metric from 802.11s draft standard [29].

Airtime link metric [30] takes into account the transmission rate, frame delivery ratio, channel access overhead and protocol overhead, defined as the default link metric to be used in WMNs. Airtime cost reflects the amount of channel resources consumed by transmitting the frame over a particular link. The airtime cost,c_a, for each link is calculated as,

$$c_a = \left[O + \frac{B_t}{r}\right] \frac{1}{1 - e_f}, \tag{42}$$

where O and B_t are defined as overhead and packet size respectively. r is the physical rate in Mbps and e_f denotes the frame error rate. Airtime metric of a path is the sum of airtime cost of each link on the path.

For comparing the performance of the three metrics, we again consider a large network of 50 nodes, but this time, we randomly select 15 source-destination pairs and their loads are varied in the range of 0.5 to 1.0 Mbps. All flows start at a random times. Each wireless link is modeled as a flat Rayleigh fading channel, with varying average link quality and error rate depending on the separation of nodes. We again employ AODV as the routing protocol in all cases.

As seen in the Fig. 27, AODV with hop count performs the worst, since the packets are always sent over the same paths that have the smallest hop count. However, as the load is increased, these paths reach saturation and data packets are dropped. The primary advantage of airtime link metric compared to hop count is that it takes into account the quality of different links. Thus, the routing protocol can choose the path with the best quality. However, the level of congestion on each path is not considered. Meanwhile, our estimated residual bandwidth metric chooses the paths according to their residual capacity that takes into account both link quality and congestion levels. Consequently, our routing protocol results in the highest end-to-end throughput due to effectively balancing the load in the network.

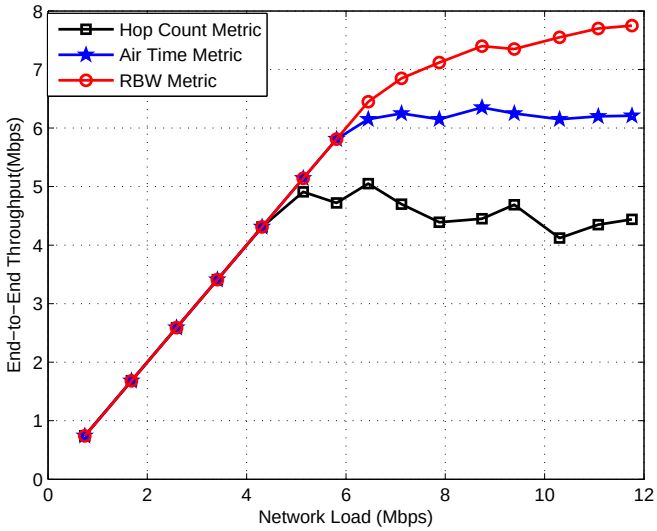

Figure 27: End-to-End Network Throughput with Different Routing Metrics

In addition, we make the same simulation for FTP application. As seen from Fig. 28, we again obtain the best performance from our estimated residual bandwidth metric. Still, routing with hop count metric has the worst performance in terms of achievable FTP throughput. Moreover, we simulate routing for CBR flows and we get the similar results with respect to contribution of routing metrics to end-to-end throughput.

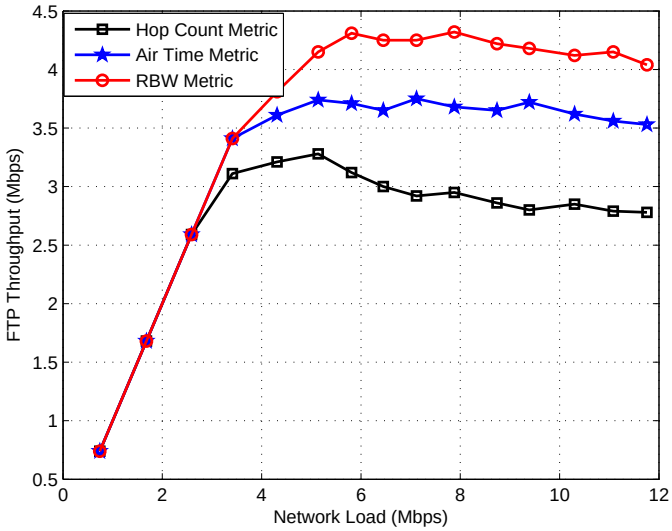

Figure 28: FTP Throughput with Different Routing Metrics

7 CONCLUSION

In this thesis, we have presented a novel method to estimate the residual bandwidth in 802.11 wireless networks under a generic WMN scenario considering all realistic conditions, hidden nodes, collisions with neighboring nodes and wireless channel impairments. Our method makes use of the measurements on link activity for building analytical models of collisions and traffic behavior. These models are then connected through the calculation of collision probability under saturation to eventually estimate the residual bandwidth.

It is proven by extensive simulation experiments that the proposed algorithm provides the most accurate residual bandwidth estimates, among existing methods, with an error margin of only 0.5-1.5%. When residual bandwidth estimates are utilized in flow admission control for WMNs, the proposed method outperforms the prominent end-to-end residual bandwidth estimation methods due to more accurate knowledge of available network capacity.

In addition, we show that when our estimated residual bandwidth is used as a routing metric, end-to-end network throughput can be significantly improved in comparison to two popular routing metrics. To the best of our knowledge, our proposed algorithm is the first residual capacity estimation method for WMNs that can simultaneously handle channel impairments, collisions and flow asymmetries. It is practically implementable in all types of 802.11 based nodes and it is applicable to a variety of network configurations to operate under different traffic loads and characteristics.

The contributions of our proposed residual bandwidth estimation algorithm can be summarized as follows:

- A novel analytical residual bandwidth estimation algorithm is proposed.
- The algorithm analyzes fading, collisions and FIM problem thoroughly.
- Our proposed algorithm has low complexity, convergence time, and high accuracy.

• The method is flexible as it can be applied in a variety of network configurations and under different traffic loads and characteristics.

• The method can be easily implemented in wireless nodes.

• By using our estimated residual bandwidth in flow admission control, packet losses are reduced significantly.

• Network aggregate throughput is increased by utilizing the estimated residual bandwidth as a routing metric.

Proposed algorithm introduces the following tolerable costs and limitations:

• Packet overhead is slightly increased due to the necessity of obtaining transmission activities of two hops away nodes. However, this overhead improves the accuracy and it is still minor compared to active methods

• The algorithm assumes that the primary link is in saturation. When the primary link reaches the saturation, this can affect the load of competing links in some cases and it affects the accuracy of the algorithm, since the load of the competing links changes.

• Our scheme does not thoroughly evaluate interference.

As future work, the interference graph can be incorporated into our model, so channel errors can be characterized more correctly. However, this approach will increase the complexity of algorithm. Also, the real implementation of the method on wireless nodes can be carried out.

References

[1] M. N. Nielsen, K. Ovsthus, and L. Landmark, "Field trials of two 802.11 residual bandwidth estimation methods," Mobile Adhoc and Sensor Systems (MASS), 2006 IEEE International Conference on, pp. 702-708, Oct. 2006.

[2] C. Sarr, C. Chaudet, G. Chelius, and I. G. Lassous, "Improving accuracy in available bandwidth estimation for ieee 802.11-based ad hoc networks," Mobile Adhoc and Sensor Systems (MASS), 2006 IEEE International Conference on, pp. 517-520, Oct. 2006.

[3] Y. Yang and R. Kravets, "Contention-aware admission control for ad hoc networks," IEEE Transactions on Mobile Computing, vol. 04, no. 4, pp. 363-377, 2005.

[4] C. S. R. Murthy and B.S.Manoj, Ad Hoc Wireless Networks. USA: Prentice Hall, 2004.

[5] P. Chung, S. C. Liew, K. C. Sha, and W. T. To, "Experimental Study of Hidden-node Problem in IEEE802.11 Wireless Networks," ACM SIGCOMM 2005, USA, 2005.

[6] K. Xu, K. Tang, M. Rajive Bagrodia; Gerla, and M. Bereschinsky, "Adaptive bandwidth management and QoS provisioning in large scale ad hoc networks," Military Communications Conference, 2003. MILCOM 2003. IEEE, vol. 2, pp. 1018-1023, Oct. 2003.

[7] L. Chen and W. Heinzelman, "Qos-aware routing based on bandwidth estimation for mobile ad hoc networks," Selected Areas in Communications, IEEE Journal on, vol. 23, no. 3, pp. 561-572, March 2005.

[8] S. Shah, K. Chen, and K. Nahrstedt, "Dynamic bandwidth management for single-hop ad hoc wireless networks," Pervasive Computing and Commu-

nications, 2003. (PerCom 2003). Proceedings of the First IEEE International Conference on, pp. 195-203, March 2003.

[9] Jin, G., Yang, G., Crowley, B., and Agarwal, D., "Network Characterization Service (NCS)," in Proceedings of 10th IEEE Symposium on High Performance Dis- tributed Computing, Aug. 2001.

[10] Ribeiro, V., Coates, M., Riedi, R., Sarvotham, S., Hendricks, B., and Bara- niuk, R., "Multifractal Cross-Traffic Estimation," in Proceedings ITC Specialist Sem- inar on IP Traffic Measurement, Modeling, and Management, Sept. 2000.

[11] Melander, B., Bjorkman, M., and Gunningberg, P., "A New End-to-End Prob- ing and Analysis Method for Estimating Bandwidth Bottlenecks," in IEEE Global Internet Symposium, 2000.

[12] Melander, B., Bjorkman, M., and Gunningberg, P., "Regression-Based Avail- able Bandwidth Measurements," in International Symposium on Performance Evalu- ation of Computer and Telecommunications Systems, 2002.

[13] Ribeiro, V., Riedi, R., Baraniuk, R., Navratil, J., and Cottrell, L., "pathChirp: Efficient Available Bandwidth Estimation for Network Paths," in Pro- ceedings of Passive and Active Measurements (PAM) workshop, Apr. 2003.

[14] G. Bianchi, "Performance analysis of the ieee 802.11 distributed coordination function," Selected Areas in Communications, IEEE Journal on, vol. 18, no. 3, pp. 535-547, Mar 2000.

[15] A. Kumar, E. Altman, D. Miorandi, and M. Goyal, "New Insights from a fixed point analysis of single cell IEEE 802.11 Wlans," Proceedings of the IEEE Infocom, March 2005.

[16] G. Sharma, A. Ganesh, and P. Key, "Performance Analysis of contention based medium access control protocols," INFOCOM 2006, 2006.

[17] C. Chaudet, I.G. Lassous, and B. Gaujal, "Study of the Impact of Asymmetry and Carrier Sense Mechanism in IEEE 802.11 Multi-hops Networks Through a Basic Case," Proc. PE-WASUN 2004, Italy, 2004.

[18] F. Daneshgaran, M. Laddomadda, F. Mesiti, and M. Modin, "A Model of the IEE 802.11 DCF in Presence of Non Ideal Transmission Channel and Capture Effects", IEEE Globecom 2007, Oct. 2007.

[19] Y. Gao, D. Chiu, and J. Lui, "Determining the End-to-End Throughput Capacity in Multi-Hop Networls: Methodology and Applications," SIGMetrics/Performance 2006, June 2006.

[20] R. Boorstyn, A. Kershenbaum, B. Maglaris, and V. Sahin, "Throughput Analysis in Multihop CSMA Packet Radio Networks," IEEE Transactions on Communications, vol. 35, no. 3, pp. 267-274, March 1987.

[21] H.S. Chaya and S. Gupta, "Performance Modeling of Asynchoronous Data Transfer Methods of IEEE 802.11 MAC Protocol," ACM Wireless Networks, vol. 3, no. 3, pp. 217-234, 1997.

[22] C. Sarr, C. Chaudet, G. Chelius, and I. G. Lassous, "Bandwidth Estimation for IEEE 802.11-Based Ad Hoc Networks," IEEE Transactions on Mobile Computing, vol. 7, no. 8, August 2008

[23] Ni Bisnik, A. Abouzeid, "Queuing Network Models for Delay Analysis of Multihop Wireless Ad Hoc Networks", IWCMC 2006, July 2006.

[24] J. Yun, S. Seo, "Novel collision detection scheme and its applications for IEEE 802.11 wireless LANs," Computer Communications Vol. 30, pp. 1350-1366, March 2007.

[25] D. Kliazovich and F. Granelli, "Cross-layer congestion control in ad hoc wireless networks," Ad Hoc Networks, vol. 4, pp. 687-708, Nov. 2006.

[26] OPNET Technologies, Inc^{TM}, Optimum Network Simulation and Engineering Too, http://www.opnet.com

[27] I.C. Atalay, Y. Sarikaya, O. Gurbuz, O. Ercetin, "Accurate Non-Intrusive Residual Bandwidth Estimation in WMNs," WiMesh 2008, 15 June.

[28] Z. Shen, R. Chen, J. G. Andrews, R. W. Heath, Jr. Member and B. L. Evans, "Low Complexity User Selection Algorithms for Multiuser MIMO Systems with Block Diagonalization," IEEE Transactions on Signal Processing, vol. 54, pp. 3658-3663, Sept. 2006.

[29] M. Pioro, P. Nilsson, E. Kubilinskas, G. Fodor, "On Efficient max-min Fair Routing Algorithms," Computers and Communication vol. 1, pp. 365-372, July 2003.

[30] IEEE 802.11 Working Group of the LAN/MAN Committee, IEEE P802.11s/DO.O1, March 2006.